Fourier-Transform Infrared Difference Spectroscopy of Rhodopsin and Its Photoproducts at Low Temperature†

Kimberly A. Bagley,‡ Valeria Balogh-Nair,§,∥ Allan A. Croteau,§,⊥ Gavin Dollinger,‡ Thomas G. Ebrey,# Laura Eisenstein,*,‡ Mi Kyung Hong,‡,# Koji Nakanishi,§ and Joseph Vittitow‡

Departments of Physics and of Physiology and Biophysics, University of Illinois at Urbana–Champaign, Urbana, Illinois 61801, and Department of Chemistry, Columbia University, New York, New York 10027

Received February 25, 1985

ABSTRACT: Fourier-transform infrared difference spectroscopy has been used to detect the vibrational modes in the chromophore and protein that change in position or intensity between rhodopsin and the photoproducts formed at low temperature (70 K), bathorhodopsin and isorhodopsin. A method has been developed to obtain infrared difference spectra between rhodopsin and bathorhodopsin, bathorhodopsin and isorhodopsin, and rhodopsin and isorhodopsin. To aid in the identification of the vibrational modes, we performed experiments on deuterated and hydrated films of native rod outer segments and rod outer segments regenerated with either retinal containing ^{13}C at carbon 15 or 15-deuterioretinal. Our infrared measurements provide independent verification of the resonance Raman result that the retinal in bathorhodopsin is distorted all-trans. The positions of the C=N stretch in the deuterated pigment and the deuterated pigments regenerated with 11-*cis*-15-deuterioretinal or 11-*cis*-retinal containing ^{13}C at carbon 15 are indicative that the Schiff-base linkage is protonated in rhodopsin, bathorhodopsin, and isorhodopsin. Furthermore, the C=N stretching frequency occurs at the same position in all three species. The data indicate that the protonated Schiff base has a C=N trans conformation in all three species. Finally, we present evidence that, even in these early stages of the rhodopsin photosequence, changes are occurring in the opsin and perhaps the associated lipids.

The absorption of light by rhodopsin, the retinal-containing protein located in the disks of the rod outer segments (ROS)[1] of vertebrate photoreceptor cells, initiates the process of vision. [For recent review, see Ottolenghi (1980), Birge (1981), and Balogh-Nair & Nakanishi (1982).] The primary amino acid sequence of bovine rhodopsin has been determined (Ovchinnikov et al., 1982; Hargrave et al., 1983), and it has been established that the retinal moiety is bound to the ϵ-amino group of lysine-296 via a Schiff-base (C=N) linkage (Shichi, 1983). After the absorption of light, in which rhodopsin is converted to the red-shifted intermediate bathorhodopsin, a series of thermal events occur (bathorhodopsin → lumirhodopsin → metarhodopsin I ↔ metarhodopsin II → metarhodopsin III → *all-trans*-retinal + opsin). This sequence initiates a change in the electrical properties of the photoreceptor cell membrane that results in the neural signal. Questions of fundamental importance are what changes in conformation of the rhodopsin molecule occur upon absorption of light and how do these changes result in production of the neural signal. To aid in answering these questions, we have employed Fourier-transform infrared (FTIR) difference spectroscopy to study changes between rhodopsin and its low-temperature photoproducts. [For a recent review of the technique of FTIR spectroscopy, see Alben & Fiamingo (1985).] This technique has been successfully applied to bacteriorhodopsin (Rothschild et al., 1981; Rothschild & Marrero, 1982; Bagley et al., 1982, 1984; Siebert & Mäntele, 1983) and to rhodopsin (Bagley et al., 1983; Rothschild et al., 1983; Siebert et al., 1983). Using this technique, we can detect those vibrational modes in the chromophore and protein moieties that change in either position or intensity upon absorption of light. To aid in the identification of these vibrational modes, we have performed experiments on deuterated and hydrated films of native ROS and ROS regenerated with retinals that contain isotopic substitutions at C-15 (Figure 1).

At low temperatures, where the thermal processes are essentially stopped, illumination of rhodopsin produces a photostationary state containing three intermediates: rhodopsin (R), bathorhodopsin (B), and isorhodopsin (I) (Yoshizawa & Wald, 1965). Chromophore extraction and regeneration of visual pigments (Walt & Brown, 1950; Hubbard & Kropf, 1958; Crouch et al., 1975), analogue studies (Akita et al., 1980), and resonance Raman studies (Callender et al., 1976; Mathies et al., 1977) have provided overwhelming evidence that the chromophore is an 11-cis conformation of retinal in rhodopsin and a 9-cis conformation in isorhodopsin. It has long been proposed that bathorhodopsin contains the all-trans isomer of retinal (Yoshizawa & Wald, 1965; Rosenfeld et al., 1977). Resonance Raman studies have since provided evidence that the chromophore is a distorted all-trans conformation in bathorhodopsin (Eyring et al., 1980, 1982). However, this result is not undisputed (Lewis, 1982). Reso-

† This work was supported in part by Grants PHS GM 32455, EY 01323, EY 07005, and EY 01253 from the Department of Health and Human Services and by Grant PCM 80-17661 from the National Science Foundation.

* Correspondence should be addressed to this author.

‡ Department of Physics.

§ Department of Chemistry.

∥ Present address: Chemistry Department, City College of New York, New York, NY 10031.

⊥ Present address: Department of Physiological Chemistry, The Ohio State University College of Medicine, Columbus, OH 43210.

Department of Physiology and Biophysics.

[1] Abbreviations: ROS, rod outer segments; FTIR, Fourier-transform infrared; IR, infrared; HOOP, hydrogen out of plane; B, bathorhodopsin; I, isorhodopsin; R, rhodopsin; Hepes, 4-(2-hydroxyethyl)-1-piperazineethanesulfonic acid.

0006-2960/85/0424-6055$01.50/0

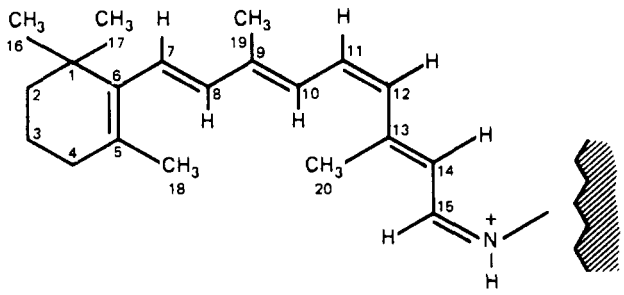

FIGURE 1: 11-*cis*,12-s-*trans*-retinal bound to opsin via a protonated Schiff-base linkage. In [15-^{13}C]retinal the carbon at position 15 is replaced by ^{13}C; in [15-^{2}H]retinal the H at carbon 15 is replaced by ^{2}H.

nance Raman studies have also shown that the protein–chromophore linkage is a protonated Schiff base in all three species (Eyring & Mathies, 1979; Aton et al., 1980; Narva & Callender, 1980) and, surprisingly, that the Schiff-base mode occurs at essentially the same frequency in all three species.

To provide new information on what occurs upon absorption of light, we have performed FTIR experiments on rhodopsin and the photostationary states that are produced at low temperature. As mentioned above, resonance Raman has been used extensively to provide information on the state of the chromophore in the various photosequence intermediates. However, resonance Raman provides little information concerning changes in the opsin during the photosequence. Infrared (IR) absorption, alternatively, is not tied to the chromophore, and therefore, changes in the protein itself can be detected. In addition, while both IR and resonance Raman measure the energy of molecular vibrations, the selection rules for the two processes are different. In fact, for molecules possessing a high degree of symmetry the two techniques are complementary; i.e., in many cases modes that are IR active are resonance Raman inactive and vice versa. In systems as complex as biological macromolecules, however, most major vibrations are expected to be both IR and resonance Raman active; however, the intensities of the modes will generally be different. We therefore argue that, in addition to providing new information on changes occurring in the opsin during the photosequence, IR can provide further information concerning the chromophore's state in the various intermediates of the photosequence.

In the absolute IR spectra of photoreceptor membranes, the chromophore vibrations are masked by the vibrational modes of the lipid, water, and polypeptide, and therefore, earlier FTIR studies have been used to obtain information on the secondary structure of rhodopsin and the orientation of the rhodopsin α-helices (Rothschild et al., 1982). However, IR difference spectroscopy can be used to detect changes occurring in the chromophore and opsin during the photosequence. Since there are three species present in the photostationary states produced at low temperatures, we have developed techniques (see Materials and Methods) for determining the relative amounts of rhodopsin, bathorhodopsin, and isorhodopsin present in each photostationary state so that the FTIR difference spectra, bathorhodopsin/rhodopsin, bathorhodopsin/isorhodopsin, and isorhodopsin/rhodopsin, could be calculated.

The resulting difference spectra provide information about the protein–chromophore linkage, isomeric state, and opsin conformation in the three species. To interpret these difference spectra, it is important to keep in mind exactly what they represent. For example, in the bathorhodopsin/isorhodopsin spectrum (Figure 2a)[2] absorptions that are entirely the same in both isorhodopsin and bathorhodopsin will cancel completely and the IR difference spectrum in that region will have zero intensity. Positive-going bands (referred to as Figure 2a+) are absorptions that occur in bathorhodopsin and occur with less intensity or not at all in isorhodopsin. Negative-going bands (referred to as Figure 2a−) are absorptions that occur in isorhodopsin and occur with less intensity or not at all in bathorhodopsin. Thus, a line that appears in bathorhodopsin does not always mean isorhodopsin has no absorption at that frequency; it could also mean that the isorhodopsin absorption is weaker than the bathorhodopsin absorption. For this reason it is helpful to examine the three possible difference spectra simultaneously to help reveal masked absorptions. The difference spectra have to be interpreted with caution. Consider the 1643- and 1649-cm^{-1} isorhodopsin lines in the B/I spectra (Figure 2a). Are these two lines for isorhodopsin, or are the two lines in Figure 2a− due to one broad line for isorhodopsin superimposed on a less intense but very sharp line for bathorhodopsin? The same problem occurs when a shoulder is observed. Common sense and intuition are necessary to examine difference spectra, and any discussion should be followed with a close examination of the spectral data.

Materials and Methods

Six types of samples were used in this study. They were H_2O and $^{2}H_2O$ suspensions of native bovine ROS fragments, bovine ROS regenerated with 11-*cis*-retinal containing ^{13}C at the carbon-15 position, and bovine ROS regenerated with 15-deuterioretinal. ROS were prepared according to the method of Papermaster & Dreyer (1974), and the opsin was prepared according to the method of Ebrey (1982).

The 11-*cis*-[15-^{13}C]retinal was prepared as follows: [1-^{13}C]acetic acid was reacted with excess isobutylene in the presence of Amberlyst 15 to provide the *tert*-butyl ester. The ester was trimethylsilylated according to Hartzell et al. (1974). Condensation with trans-cis C-18 ketone provided 11-*cis*- and 11-*cis*, 13-*cis*-*tert*-butyl retinoate. The ester was reduced to the alcohol with diisobutylaluminum hydride and then oxidized to the retinal with MnO_2. Although 11-cis is the minor isomer, the remaining material can be converted to a mixture containing 35% 11-cis by 514.5-nm laser photolysis on silica gel in cyclohexane (Zawadski & Ellis, 1983), recycling repeated as necessary. 11-*cis*-[15-^{2}H]Retinal was prepared as follows: Methyl retinoate was prepared from retinoic acid with CH_3I and 1,8-diazobicyclo[5.4.0]undec-7-ene (DBU) (Ono et al., 1978); reduction of the ester with $LiAlD_4$ (Et_2O, −10 °C) followed by MnO_2 oxidation yielded *trans*-[15-^{2}H]retinal. Laser photolysis at 514.5 nm provided a [15-^{2}H]retinal mixture containing 35% 11-cis, the remaining isomers recycled as necessary.

Pigments were regenerated from bleached rod outer segment membranes suspended in 10 mM pH 7.0 Hepes buffer at 22 °C by addition of retinal analogues. The regenerated pigments were washed with 10 mM Hepes buffer at 22 °C to remove unbound retinal and then concentrated to ca. 5 OD/mL (at 495 nm) for film formation. Deuteration was carried out by incubation of lyophylized pigments with 99.9% $^{2}H_2O$ several times.

[2] No corrections have been made for the small variations in sample thickness and concentration from experiment to experiment or for the changes in scale resulting from different photostationary-state combinations used to extract the pure difference spectra for different experiments. For example, with the results in Table I, the combination (460/570) + 0.8(520/650) yields 0.80 B/I, whereas the combination (460/570) + 0.186(570/*R*) yields 0.55 B/I.

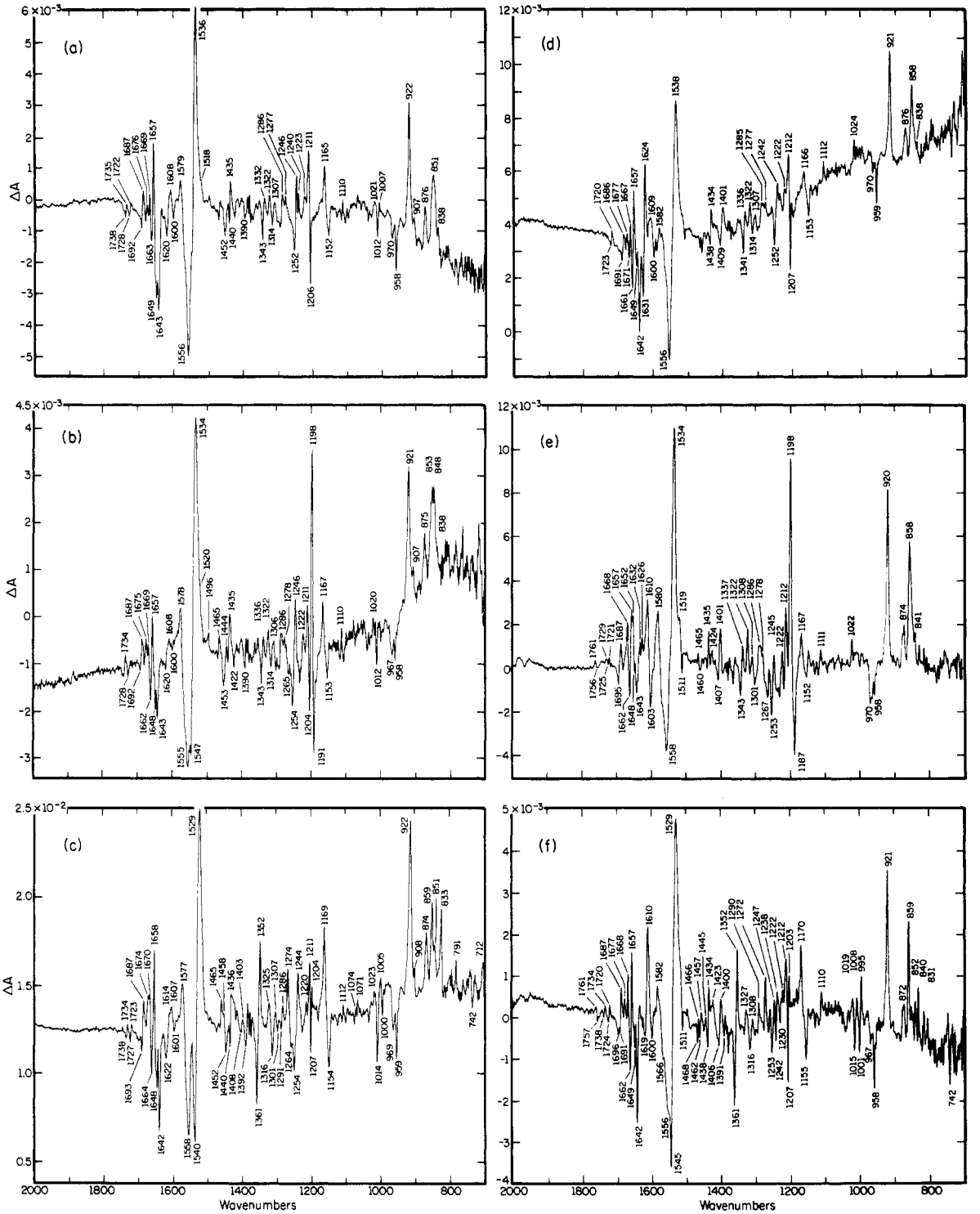

FIGURE 2: FTIR difference spectra between bathorhodopsin and isorhodopsin, bathorhodopsin/isorhodopsin at 70 K. The difference spectra were calculated by subtracting photostationary-state difference spectra with appropriate weighting factors (calculated from the concentrations given in Table I). Note: due to the nature of these subtractions, the scales given in these spectra are somewhat arbitrary. Resolution is 2 cm^{-1}. (a) Hydrated film of ROS; (b) hydrated film of ROS containing rhodopsin regenerated with 11-*cis*-[15-^{13}C]retinal; (c) hydrated film of ROS containing rhodopsin regenerated with 11-*cis*-[15-^{2}H]retinal; (d) deuterated film of ROS; (e) deuterated film of ROS containing rhodopsin regenerated with 11-*cis*-[15-^{13}C]retinal; (f) deuterated film of ROS containing rhodopsin regenerated with 11-*cis*-[15-^{2}H]retinal.

The samples were dried under a vacuum onto an IR transmitting but visibly opaque window of germanium. The film was vacuum sealed with NaCl as the second window. The films were not purposely hydrated since comparable experiments done on films exposed to an atmosphere of 98% humidity and then sealed showed no significant differences between the spectra for the two systems. Henceforth, we refer to these films as hydrated films. To ensure the integrity of the deuterated films, a small amount of $^{2}H_2O$ was added to the periphery of the film. The absorbance of the films was approximately 0.1 OD at 500 nm.

The film was then mounted in a helium refrigerator equipped with NaCl windows. A Nicolet 7199 FTIR spectrometer with a HgCdTe detector was used to record spectra. To filter out the incident visible radiation from the IR source and yet illuminate the sample from the other side with visible light during the course of the experiment, the germanium window was mounted so that the side the film was on faced

Table I: Percentages, Determined by High-Pressure Liquid Chromotography, of Rhodopsin, Isorhodopsin, and Bathorhodopsin in Photostationary States[a]

λ (nm)	% rhodopsin (11-cis)	% isorhodopsin (9-cis)	% batho-rhodopsin (all-trans)
460	26.7	18.5	54.8
520	31.5	29.4	39.1
570	9.9	90.1	0.0
650[b]	52.5	40.5	7.0
no light	100.0	0.0	0.0

[a] The photostationary states were created with 460-, 570-, 520-, and 650-nm light from a projector equipped with interference filters. The order in which the sample was irradiated was 460 nm, followed by 570, 520, and finally 650 nm. The photostationary states were always created in the same order. The results are the same in ^2H_2O. The errors in the percentages are less than 3%. There is excellent agreement between these results and those of Suzuki & Callender (1981) for the photostationary state mixtures. [b] We refer to the states produced by light as photostationary states and checked that no further changes in the FTIR spectra occurred when the samples were illuminated twice as long. However, if a true photostationary state is not achieved, as would be the case for wavelengths for which an extremely long illumination time would be necessary to reach the photostationary state, none of the results in this paper would be changed. Since the data are always taken under the same experimental condition, it would just mean that for that particular wavelength of illumination the mixture produced is as given in this table.

away from the IR source.

The sample was cooled to 70 K, and an IR transmission spectrum was collected over the region 4900–700 cm^{-1}. To eliminate base-line drift, 512 scans were collected from the sample, 512 scans were collected as background from a compartment containing no sample, and the ratio of the sample to the background was calculated. This process was repeated until four successive difference spectra had been collected. The four spectra were then averaged, resulting in a 2-cm^{-1} resolution transmission spectrum with an adequate signal-to-noise ratio.

Four illumination wavelengths were used to create photostationary states. The relative concentrations of each species in these photostationary states were determined by warming the sample to room temperature in the dark, resuspending it in hydroxylamine (2.0 M), and analyzing the isomers present by high-performance liquid chromatography (Table I). Upon warming, bathorhodopsin goes through the bleaching sequence producing *all-trans*-retinal. Thus, the relative concentrations of rhodopsin, bathorhodopsin, and isorhodopsin present in each photostationary state are given by the relative concentrations of 11-cis, all-trans, and 9-cis obtained from high-performance liquid chromatography. As can be seen from Table I, illumination with 570-nm light creates a photostationary state that contains a large percentage of isorhodopsin and no bathorhodopsin. Therefore, an IR difference spectrum between isorhodopsin and rhodopsin can be obtained directly. Unfortunately, one cannot obtain a bathorhodopsin/rhodopsin or bathorhodopsin/isorhodopsin spectrum in this manner. However, by subtracting photostationary-state difference spectra with appropriate weighting factors (calculated from the concentrations given in Table I), we have obtained bathorhodopsin/isorhodopsin and bathorhodopsin/rhodopsin IR difference spectra. As a check on the reliability of these spectra, we performed subtractions using different combinations of the original photostationary-state difference spectra, and identical results were obtained. The IR vibrational frequencies given in this paper are those that occur in the difference spectra. No corrections have been made for the distortions in the shape and location of peaks that occur when difference spectra are calculated, nor were the spectra smoothed.

One must be careful in comparing intensities of lines from run to run, since in regions of the spectra having high absolute absorption, i.e., amide A (~3300 cm^{-1}), amide I (~1660 cm^{-1}), amide II (~1550 cm^{-1}), and amide III (~1270 cm^{-1}), small changes in humidity and/or temperature can result in changes in the base line of the difference spectra in these regions. These changes in base line result in apparent changes in intensity for those lines in the difference spectra. The protein bands above 2000 cm^{-1} are obscured by H_2O or ^2H_2O; therefore, only data below 2000 cm^{-1} are presented in this paper.

The bathorhodopsin/isorhodopsin spectra are shown in Figure 2, the bathorhodopsin/rhodopsin spectra in Figure 3, and the isorhodopsin/rhodopsin spectra in Figure 4.

Results

Spectral Region between 1800 and 1700 cm^{-1}. Several lines are observed in the IR difference spectra above 1700 cm^{-1}. Although weak, these lines are reproducible and appear in a region that is not complicated by chromophore absorptions. It is in this region that the carbonyl stretching frequencies of carboxyl and ester groups appear (~1710–1780 cm^{-1}) and aromatic amino acids such as tyrosine, phenylalanine, and tryptophan show overtone and combination bands (2000–1660 cm^{-1}) (Nakanishi & Solomon, 1977).

In the region above 1750 cm^{-1} the bathorhodopsin/rhodopsin difference spectra show the cleanest lines (Figure 3). For hydrated ROS, a 1772-cm^{-1} bathorhodopsin line (Figure 3a+) and a 1770-cm^{-1} rhodopsin line (Figure 3a–) are observed in agreement with previously published IR results for rhodopsin and bathorhodopsin (Siebert et al., 1983). The position of these lines is insensitive to ^{13}C or ^2H substitution at C-15 of the retinal moiety (Figure 3b,c). However, upon deuteration of the medium both lines shift: bathorhodopsin to 1762 cm^{-1} (Figure 3e+) and rhodopsin to 1756 cm^{-1} (Figure 3e–). It is therefore likely that these lines arise from changes associated with –COOH (–COO^2H) groups of aspartic or glutamic acid residues (Nakanishi & Solomon, 1977). Similar changes have been observed in the early stages of the bacteriorhodopsin photocycle; in the transition of bacteriorhodopsin to K, the bathorhodopsin-like intermediate in the bacteriorhodopsin system, a shift from 1741 to 1733 cm^{-1} was observed (Bagley et al., 1984). These bands were also found to be independent of isotopic substitutions at C-15 of the chromophore, but both bands shifted to lower wavenumbers by about 10 cm^{-1} upon deuteration of the medium.

These lines can result from a change in environment of a carboxylic group or from the simultaneous deprotonation of one carboxylic group along with the protonation of a second carboxylate. Identification of changes in carbonyl stretching frequencies of carboxylates, which occur at lower wavenumbers (1610–1550 cm^{-1} for the antisymmetric combination, 1400 cm^{-1} for the symmetric combination), would establish the involvement of two or more carboxylic groups in the rhodopsin (bacteriorhodopsin) to bathorhodopsin (K) transition. Such an interpretation is attractive since it could explain the previously observed medium deuteration effects in the kinetics of the rhodopsin (bacteriorhodopsin) to bathorhodopsin (K) transition at low temperature (Peters et al., 1977; Applebury et al., 1978).

The B/I difference spectra (Figure 2a–c) show bathorhodopsin lines at 1722 and 1735 cm^{-1} (Figure 2a+, 2b+, 2c+) and isorhodopsin lines at 1728 and 1738 cm^{-1} (Figure 2a–, 2b–, 2c–). The B/R difference spectra (Figure 3a–c) also

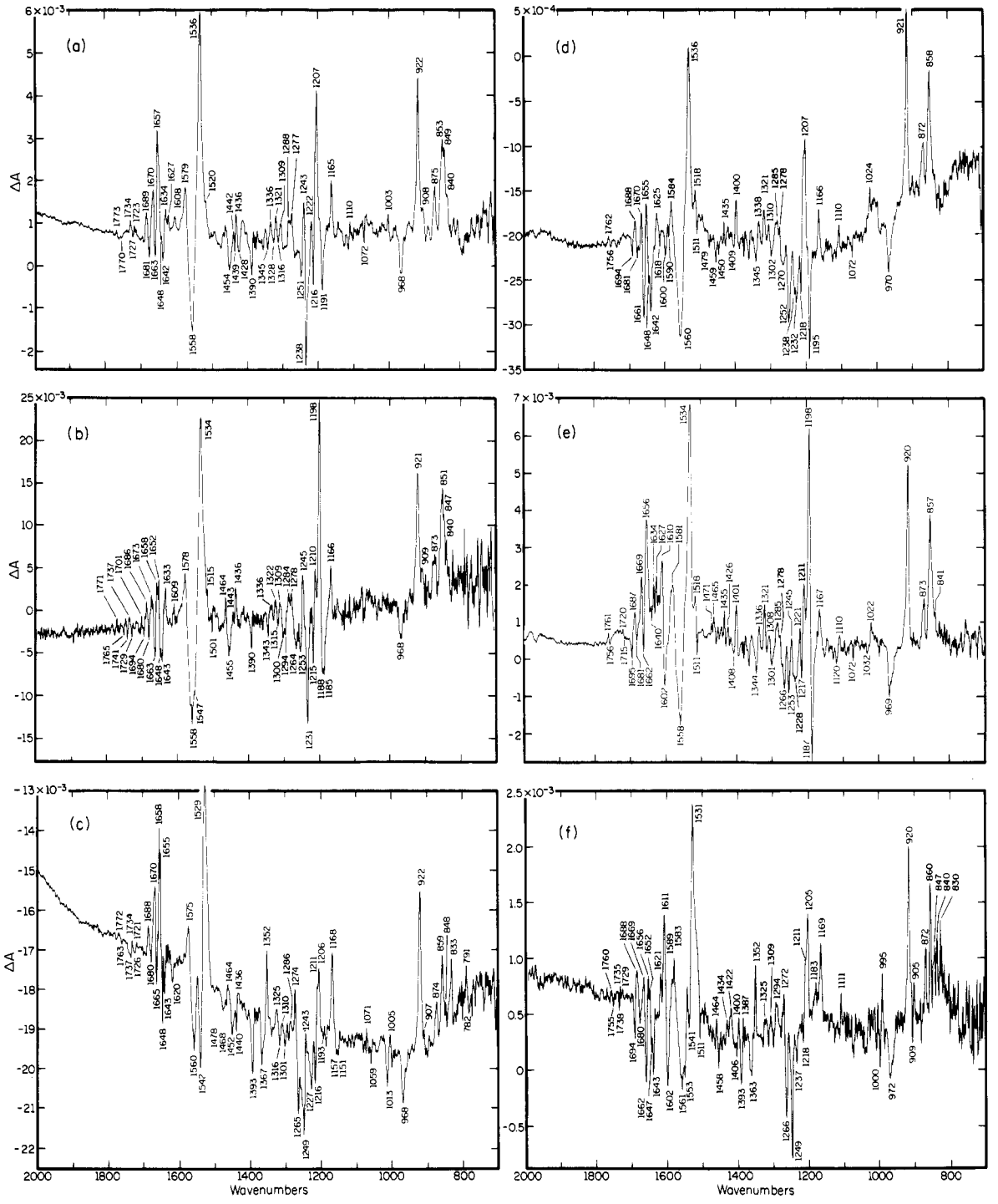

FIGURE 3: FTIR difference spectra between bathorhodopsin and rhodopsin, bathorhodopsin/rhodopsin at 70 K. Note: due to the nature of these subtractions the scales given in these spectra are somewhat arbitrary. Resolution is 2 cm^{-1}. (a) hydrated film of ROS; (b) hydrated film of ROS containing rhodopsin regenerated with 11-*cis*-[15-^{13}C]retinal; (c) hydrated film of ROS containing rhodopsin regenerated with 11-*cis*-[15-^{2}H]retinal; (d) deuterated film of ROS (e) deuterated film of ROS containing rhodopsin regenerated with 11-*cis*-[15-^{2}H]retinal; (f) deuterated film of ROS containing rhodopsin regenerated with 11-*cis*-[15-^{2}H]retinal.

show the 1722- and 1735-cm^{-1} bathorhodopsin lines (Figure 3a+, 3b+, 3c+) and rhodopsin lines at 1728 and 1741 cm^{-1} (Figure 3a–, 3b–, 3c–). The positions of all of these lines are insensitive to medium deuteration (Figures 2d–f and 3d–f), and hence, these lines probably reflect changes in the environment of the ester groups in the lipid or nonexchangeable carboxylic (aspartic or glutamic) residues buried in the protein. However, it is also possible that these lines reflect subtle changes in the overtone and combination bands of the aromatic amino acids. Such lines in the 1745–1725-cm^{-1} region of the spectrum, which do not shift upon medium deuteration, have not been observed in the bacteriorhodopsin system (Bagley et al., 1984). Bacteriorhodopsin is obtained from the archaebacterium *Halobacterium halobium*, whose lipids are distinguished from those of procaryotes and eucaryotes by the absence of fatty acid glycerol ester lipids (Kates & Kushawa, 1978; Langworthy et al., 1982). Thus, it is tempting to associate these lines in ROS with the ester groups of their lipids. This would imply changes in lipids during the early stages of the photobleaching sequence.

Spectral Region between 1700 and 1600 cm^{-1} (Tables II and III). In the 1700–1600-cm^{-1} region of the IR spectra,

Table II: Spectral Region between 1700 and 1600 cm^{-1}

		native[c]				15-^{13}C[d]				15-^{2}H[e]			
		B/I[f]		B/R		B/I		B/R		B/I		B/R	
species[a]	medium[b]	figure[g]	lines (cm^{-1})[h]	figure	lines (cm^{-1})	figure	lines (cm^{-1})	figure	lines (cm^{-1})	figure	lines (cm^{-1})	figure	lines (cm^{-1})
batho-rhodopsin (B)	H_2O	2a+	1687, 1676, 1669, 1657, 1608	3a+	1689, (1677), 1670, 1657, 1634, 1627, 1608	2b+	1687, 1675, 1669, 1657, 1608	3b+	1686, 1673, 1658, 1652, 1633, 1609	2c+	1687, 1674, 1670, 1658, 1614, 1607	3c+	1688, (1677), 1670, 1658, 1655
	$^{2}H_2O$	2d+	1686, 1677, 1667, 16578 1624*, 1609	3d+	1688, (1677), 1670, 1655, 1625*	2e+	1687, (1677), 1668, 1657, 1652, 1632, *1626*, 1610	3e+	1687, (1677), 1669, 1656, 1634, 1627, 1610*	2f+	1687, 1677, 1668, 1657, 1610*	3f+	1688, (1677), 1669, 1656, 1652, 1621, 1611*

		native[c]				15-^{13}C[d]				15-^{2}H[e]			
		B/I[f]		I/R		B/I		I/R		B/I		I/R	
species[a]	medium[b]	figure[g]	line (cm^{-1})[h]	figure	lines (cm^{-1})	figure	lines (cm^{-1})	figure	lines (cm^{-1})	figure	lines (cm^{-1})	figure	lines (cm^{-1})
iso-rhodopsin (I)	H_2O	2a-	1692, (1671), 1663, 1649, 1643, 1620, 1600	4a+	1691, 1671, (1663), 1652, 1642, 1620, 1601	2b-	1692, (1671), 1662, 1648, 1643, 1620, 1600	4b+	1692, 1670, (1662), 1652, 1640, 1600	2c-	1693, (1670), 1664, 1648, 1642, 1622, 1601	4c+	1691, 1668, 1655, 1644, 1633, 1626, 1600
	$^{2}H_2O$	2d-	1691, 1671, 1661, 1649, 1642, 1631*, 1600	4d+	1691, 1670, (1661), 1653, 1642, 1631	2e-	1695, (1970), 1662, 1648, 1643, 1603*	4e+	1691, 1671, (1662), 1654, 1642, 1621, 1612, (1603*)	2f-	1696, 1691, (1671), 1662, 1649, 1642, (1619), (1614*), 1600	4f+	1690, 1671, (1662), 1652, 1641, 1621, 1614*

		native[c]				15-^{13}C[d]				15-^{2}H[e]			
		B/R		I/R		B/R		I/R		B/R		I/R	
species[a]	medium[b]	figure[g]	lines (cm^{-1})[h]	figure[g]	lines (cm^{-1})	figure	lines (cm^{-1})	figure	lines (cm^{-1})	figure	lines (cm^{-1})	figure	lines (cm^{-1})
rhodopsin (R)	H_2O	3a-	(1693), 1681, 1663, 1648, 1642	4a-	1693, 1679, (1663), (1648), (1642), 1611	3b-	1694, 1680, 1663, 1648, 1643	4b-	(1694), (1680), 1665, 1657, 1647, 1613, 1608	3c-	1680, 1665, 1648, 1643, 1620	4c-	1680, 1666, 1648, 1636, 1630
	$^{2}H_2O$	3d-	1694, 1681, 1661, 1648, 1642, (1624*), 1618, 1600	4d-	(1684), 1677, 1665, 1658, (1642), 1624*	3e-	1695, 1681, 1662, 1640, 1602*	4e-	1694, 1678, 1666, 1659, 1649, 1635, 1603*	3f-	1694, 1680, 1662, 1647, 1643, 1602*	4f-	1694, 1679, 1665, 1657, 1646, 1634, 1603*

[a] The measured intermediate in the photosequence. [b] The media in which the ROS were suspended. The ROS suspended in H_2O yield hydrated films whereas the $^{2}H_2O$ media suspended ROS yield deuterated films. [c] Native ROS. [d] Pigments containing [15-^{13}C]retinal. [e] Pigments containing [15-^{2}H]retinal. [f] For example, B/I means the difference IR spectrum between B and I. [g] The (+) and (-) signs denote respectively the positive and negative sides of the difference spectra in the figures. [h] Lines quoted in the text that are assigned to the C=N stretching frequency are marked with an asterisk; lines which are weak and not discussed in the text are underlined; if the line is assigned in the text as belonging to a particular species but does not appear in both possible difference spectra, the line appears in parentheses for the figure in which it does not appear.

the C=N stretching frequency due to the Schiff-base linkage of the chromophore is expected to appear together with some C=C stretches (below approximately 1630 cm^{-1}). In addition, the opsin has a strong amide I line ($\nu_{C=O}$) centered at 1660 cm^{-1}, and hence, the difference spectra may also reflect subtle changes in peptidic amide bonds. In fact, this region of the IR spectra shows many more lines than can be attributed to changes in the C=N stretching frequency of the chromophore between any two of the species. Data are shown in Figures 2–4 and Table II. Our assignments of C=N stretching frequencies in native and analogue pigments are summarized in Table III.

The following lines can be assigned to the respective species from the various difference spectra: bathorhodopsin (B)

Table III: IR Lines (cm^{-1}) Assigned to C=N Stretch for Bathorhodopsin, Isorhodopsin, and Rhodopsin in Hydrated and Deuterated Native and Analogue ROS

species	HC=NH	HC=N^{2}H	H^{13}C=NH	H^{13}C=N^{2}H	^{2}HC=NH	^{2}HC=N^{2}H
bathorhodopsin	(1659)[a]	1624	*x*[b]	1610	*y*[c]	1610
isorhodopsin	(1659)	1631	*x*	1603	*y*	1614
rhodopsin	(1659)	1624	*x*	1602	*y*	1602
PSB in MeOH[d]	1656	1632	1637	1614	1641	1618
PSB in CH_2Cl_2[d]	1653	1632	1632	1612	1639	1618
bacteriorhodopsin[e]	1639	1627	1629	1610	1632	1614

[a] IR results are consistent with this resonance Raman assignment; however, no direct evidence from IR difference spectra supports this assignment. The 1657-cm^{-1} B line in the IR difference spectra is probably due to small changes in the opsin. [b] IR difference spectra only provide evidence that in all three species (B, I, R) the hydrated 15-^{13}C-labeled analogue lines are in the same location. The shift of the C=N stretch between hydrated ROS and hydrated 15-^{13}C-labeled analogue is undetermined. [c] As in the 15-^{13}C case the shift in hydrated 15-^{2}H is undetermined. IR difference spectra only provide evidence that the ^{2}HC=NH stretch is in the same location in B, I, and R. [d] Protonated butylamine Schiff base, A. A. Croteau and K. Nakanishi, unpublished results. [e] Data from Bagley et al. (1984).

(Figures 2a+ and 3a+), 1687, 1676, 1669, and 1657 cm^{-1}; isorhodopsin (I) (Figures 2a– and 4a+), 1692, 1671, 1663, 1649, and 1643 cm^{-1};[3] Rhodopsin (R) (Figures 3a– and 4a–), 1693, 1681, 1663, 1648, and 1642 cm^{-1}.[3]

By observation of line shifts upon deuteration of the medium, resonance Raman studies were able to identify the C=N stretching frequency in B, I, and R as 1659 cm^{-1} and to interpret the deuteration shifts as arising from protonated Schiff-base linkages in all three species (Lewis et al., 1973; Oseroff & Callender, 1974; Mathies et al., 1976; Callender et al., 1976; Eyring & Mathies, 1979; Narva & Callender, 1980). Similarly, the IR line for each species due to the C=NH stretch is expected to disappear upon deuteration and/or isotopic substitution at C-15, and in each case a new line should appear. However, it was found that no IR line in the hydrated spectra disappears upon medium deuteration or isotopic substitution at C-15; e.g., compare Figure 2a+ with Figure 2b+, 2c+, 2d+, 2e+, 2f+. Furthermore, it is not possible to state with certainty whether there are significant changes in the intensity of any single line upon deuteration of ROS or isotopic substitution at C-15. The changes in line intensities in this region that have been observed for hydrated ROS preparations from experiment to experiment probably arose from overall changes in the amide I band intensity.

The observation that no line in this region of the hydrated ROS spectra disappears upon deuteration can be interpreted by assuming the following: the bands of B, I, and R that should be shifted upon deuteration are all in the same position and therefore cancel out and are observable. This explanation agrees with the resonance Raman results where the C=N mode of all three species was assigned to bands at the same location. Furthermore, no new lines appear in the hydrated spectra upon isotopic substitution at C-15 by ^{13}C or by ^{2}H: i.e., 15-^{13}C and 15-^{2}H analogues of B (Figure 2b+, 2c+, compare with Figure 2a+), I (Figure 2b–, 2c–, compare with Figure 2a–), and R (Figure 3b–, 3c–, compare with Figure 3a–). We explain the absence of new lines in these cases by assuming that the bands shifted by isotopic substitutions are shifted to the same locations for B, I, and R.

[3] The 1643/1642-cm^{-1} line has been assigned as both an isorhodopsin line and a rhodopsin line since it appears in Figures 2a+ and 3a–. However, the line also appears as an isorhodopsin line (Figure 4a+) in the I/R spectra. This apparent contradiction is explained by the assumption that the line belongs to both I and R but is more intense in I. Similar arguments are used for many of the assignments presented in this article. All such cases are denoted in the tables as follows: if the line is assigned as belonging to a particular species but does not appear in both possible IR difference spectra, the line appears in parentheses for the figure in which it does not appear (see Table II); e.g., for R, 1642 cm^{-1} appears as (1642) in Figure 4a–.

In all cases where the experiments were done in deuterated media, however, new lines are observed in the 1700–1600-cm^{-1} region. For B in deuterated ROS (Figures 2d+ and 3d+), a new line appears at 1624 cm^{-1}; similarly, a new line is observed for I at 1631 cm^{-1} (Figures 2d– and 4d+) and for R at 1624 cm^{-1} (Figure 4d–, but not seen in Figure 3d–). These frequencies are in agreement with the results of IR studies carried out by Siebert et al. (1983).

In the case of the 15-^{13}C analogue, the medium-deuterated species of B is characterized by a line at 1610 cm^{-1} (Figures 2e+ and 3e+) and of R by a line at 1602 cm^{-1} (Figure 3e– and 4e–). For isorhodopsin, the B/I difference spectrum (Figure 2e–) reveals a line at 1603 cm^{-1}, but the I/R difference spectrum (Figure 4e+) reveals two new lines at 1621 and 1612 cm^{-1} but none around 1603 cm^{-1}. Since rhodopsin is characterized by strong lines at 1603 cm^{-1} in the B/R and I/R difference spectra (Figure 3e– and 4e–), the absence of a 1603-cm^{-1} line for I in the I/R difference spectrum is not surprising if the 1603-cm^{-1} line for R is more intense than that of I. However, the two I lines at 1621 and 1612 cm^{-1} are not readily accounted for.

Similar results are encountered for the medium-deuterated 15-^{2}H-labeled analogues. B has a 1610-cm^{-1} line (Figures 2f+ and 3f+), while spectra for R show a 1602-cm^{-1} line (Figures 3f– and 4f–). In the case of I, the I/R spectrum (Figure 4f+) again shows lines at 1621 and 1614 cm^{-1} [as with the I/R difference spectrum (Figure 4e+)]; however, no new I line is observable in the B/I spectrum (Figure 2f–). It may be that in the medium-deuterated 15-^{2}H-labeled analogues the new I line is around 1610 cm^{-1} but it is not apparent in the B/I spectrum (Figure 2f–) because B has a stronger absorption in this region as seen by the strong 1610-cm^{-1} lines in B/I spectrum (Figure 2f+) and B/R spectrum (Figure 3f+).

Isotopic substitution at C-15 leads to no new lines in the hydrated species of B, I, and R; however, in the medium-deuterated species characteristic lines appear upon isotopic substitution (Table III). This different behavior is difficult to reconcile except for assuming that in the hydrated species the bands shift to the same location in all three species (B, I, and R; see above) while in the deuterated cases they do not. Nonetheless, the shifting patterns in the deuterated cases indicate that these lines for all three intermediates are associated with a protonated Schiff-base linkage. The argument is as follows. Any shifts upon deuteration in this region of the spectra can result from only two sources: a protonated Schiff-base linkage or some protonated site on the protein. Since, however, the lines in B, I, and R appear at different locations in deuterated ROS, deuterated 15-^{13}C-labeled ROS, and 15-^{2}H-labeled ROS, the lines are associated with the chromophoric moeity and not the protein. In addition, the size of the shifts and the location of the lines in deuterated ROS

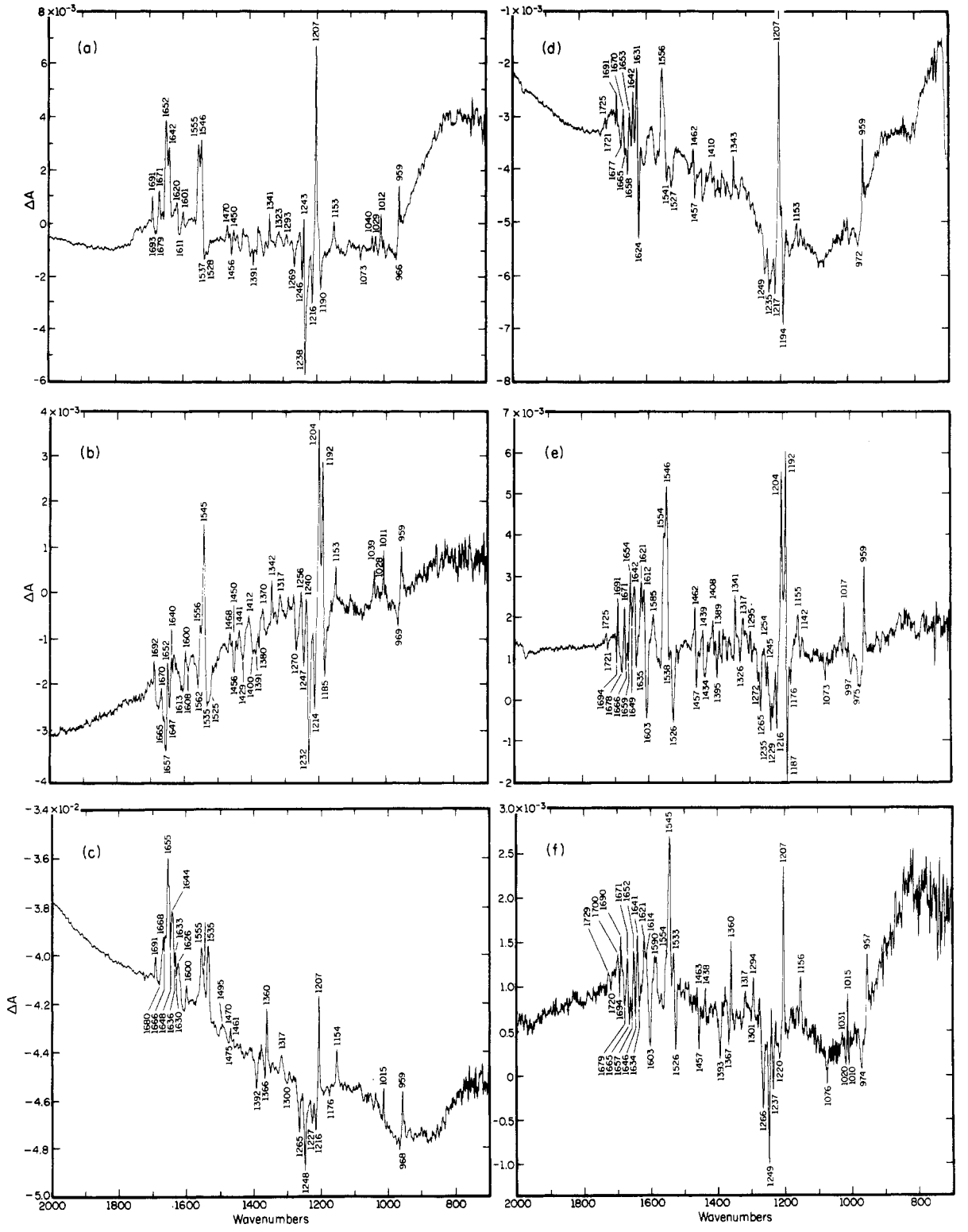

FIGURE 4: FTIR difference spectra between isorhodopsin and rhodopsin, isorhodopsin/rhodopsin at 70 K. The difference spectra were obtained either by subtraction of the rhodopsin IR spectra (no light) from the 570-nm photostationary-state IR spectra or from calculations using photostationary-state studies. Note: due to the nature of these subtractions the scales given in these spectra are somewhat arbitrary. Resolution is 2 cm^{-1}. (a) Hydrated film of ROS; (b) hydrated film of ROS containing rhodopsin regenerated with 11-*cis*-[15-^{13}C]retinal; (c) hydrated film of ROS containing rhodopsin regenerated with 11-*cis*-[15-^{2}H]retinal; (d) deuterated film of ROS; (e) deuterated film of ROS containing rhodopsin regenerated with 11-*cis*-[15-^{2}H]retinal; (f) deuterated film of ROS containing rhodopsin regenerated with 11-*cis*-[15-^{2}H]retinal.

and the deuterated analogues of ROS agree favorably with the values obtained from IR measurements of both deuterated butylamine Schiff bases of *all-trans*-retinal and analogues (A. A. Croteau and K. Nakanishi, unpublished results) and of deuterated bacteriorhodopsin (Bagley et al., 1984), for which a protonated Schiff-base linkage has been established (Table III). We thus conclude that these shifting patterns result from protonated Schiff-base linkages in bathorhodopsin, isorhodopsin, and rhodopsin.

Protonated retinylidene Schiff bases exhibit Schiff-base stretching frequencies in the range 1660–1640 cm^{-1} [Lewis (1982) and references cited therein]. The Schiff-base vibrational mode in protonated Schiff bases of retinal and pigments involves the coupled motion of the C=N stretch and the N–H

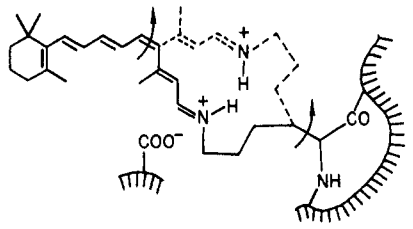

FIGURE 5: Hypothetical scheme depicting the conversion of rhodopsin (heavy line) to bathorhodopsin (dotted line); the figure is depicted in a two-dimensional rather than a three-dimensional manner, and hence, the carboxylate group and the hydrogen of the protonated Schiff base are depicted as facing away from each other, which should not be the case. The protonated Schiff-base linkage is depicted in the anti form rather than the syn form (see text).

and 15-H in-plane bends (Aton et al., 1980; Kakitani et al., 1983). It is the coupling of the C=N stretch to the C-N-H bend that is responsible for the shift to higher frequencies in protonated Schiff bases as compared to nonprotonated Schiff bases. The coupling pushes the high-frequency vibrational mode ($\nu_{C=N}$) to higher frequencies and the low-frequency vibrational mode (δ_{C-N-H}) to lower frequencies than would be observed if these vibrations were not coupled. Since the extent of coupling is larger when these two vibrations are closer, medium deuteration essentially removes the coupling by lowering the δ_{C-N-H} from ca. 1350 to ca. 1000 cm^{-1} (δ_{C-N-^2H}). Thus, deuteration at the C-15 and N positions results in an uncoupled C=N stretch, which is at a lower frequency (close to the "pure" $\nu_{C=N}$).

The 1654-cm^{-1} line in protonated Schiff bases of *all-trans*-retinal has been assigned to a normal mode involving the C=N stretch, the C-14/C-15 stretch, and the 15-H and N-H bends (Smith et al., 1985). Deuteration at both the C-15 and N positions results in a normal mode, which essentially only involves the C=N and 14–15 stretches. Since the dominant contribution to the Schiff base normal mode is due to the C=N stretch (Smith et al., 1985), the frequency obtained for the 15-deuterio analogue in deuterated media should be approximately that of the pure C=N stretch. Table III (last column) shows that the frequencies of this pure C=N stretch in bathorhodopsin, rhodopsin, and isorhodopsin are 1610, 1602, and 1614 cm^{-1}, respectively. That these values are all different implies that the C=N force constant is different in all three species. This is reasonable, since the environment near the Schiff-base end of the chromophore is expected to be different for each species (see Figure 5).

It is interesting to note that the values obtained for bathorhodopsin (1610 cm^{-1}), isorhodopsin (1614 cm^{-1}), bacteriorhodopsin (1614 cm^{-1}) and *all-trans*-retinal protonated Schiff base (1618 cm^{-1}) are all similar, while that for rhodopsin (1602 cm^{-1}) is considerably lower. That the pure C=N stretch is lower in frequency in rhodopsin than in bacteriorhodopsin or protonated Schiff bases is consistent with expectations on the basis of point-charge models (Honig et al., 1979). Kakitani et al. (1983) pointed out that the external charge near C-12 of the chromophore in rhodopsin should result in a major increase in the π-electron delocalization near the Schiff-base terminus of the chain and thus a lower C=N force constant for rhodopsin. However, their calculations were unable to reproduce this expectation. Instead, for the 15-deuterio analogue in deuterated media their calculations gave a slightly higher Schiff-base frequency for rhodopsin than for bacteriorhodopsin (1619 cm^{-1} in rhodopsin and 1613 cm^{-1} in bacteriorhodopsin). However, the rhodopsin and bacteriorhodopsin calculated frequencies are at least closer than they were for the case of native pigments in H_2O in which the rhodopsin Schiff-base frequency is considerably higher (1657 cm^{-1} in rhodopsin and 1642 cm^{-1} in bacteriorhodopsin).

The fact that the frequencies of the Schiff-base mode in hydrated media are the same for bathorhodopsin, isorhodopsin, and rhodopsin implies that the N-H bend makes an important contribution to this normal mode and that the frequency of the N-H bend and/or the coupling of the N-H bend to the C=N stretch is considerably different in all three species. Their presence is necessary to explain how pure C=N stretches of different frequencies can be shifted to normal modes of the same frequency. Differences in the diagonal and coupling force constants for the C-N-H bending vibrations are not unexpected. Differences in the strength and geometry of hydrogen bonds and salt bridges formed by the Schiff base and charge density of the Schiff-base nitrogen would result in different C=N, N-H, and C-N-H force constants and coupling constants in all three species. What is surprising is that all these effects result in vibrational modes of the same frequency in hydrated media for bathorhodopsin, isorhodopsin, and rhodopsin. The C=N vibrational modes of the 15-^{13}C and 15-^{2}H analogues of B, I, and R are again at the same frequencies in hydrated media (but not in deuterated media). Normal mode calculations are now in progress to elucidate these unexpected results.

As noted above, many lines appear in the 1700–1600-cm^{-1} region of the IR difference spectra between B, I, and R in hydrated native ROS, none of which arise from the Schiff-base stretching frequency. Furthermore, these lines have not been detected in resonance Raman studies, and their positions are insensitive to deuteration of the medium and/or isotopic substitution at C-15. In this region of the spectrum (above approximately 1630 cm^{-1}), the only chromophore line expected to appear is the C=N stretch. We therefore conclude that the lines detected in this region result from changes in the apoprotein. Since amide I has a broad absorption at ca. 1660 cm^{-1} and is insensitive to deuteration of ROS, we propose that lines detected in this region of the IR spectra result from small changes in environment of amide bonds located near the chromophore pocket. More specifically, it seems reasonable to expect that a change in conformation of the chromophore (for instance, isomerization around the 11–12 double bond in the rhodopsin to bathorhodopsin transition) would result in small changes in the environment of the amides to which lysine-296 is linked (see Figure 5).

Spectral Region between 1600 and 1500 cm^{-1} (Table IV). The only vibrational modes of the chromophore that are expected to appear in the spectral region between 1600 and 1500 cm^{-1} are the ethylenic C=C stretches. Also appearing in this region are the broad amide II band (C-N stretch coupled with N-H bend) of the opsin, which peaks at 1550 cm^{-1}, skeletal stretches associated with aromatic amino acid residues of the opsin, and the antisymmetric carbonyl mode of carboxylate residues in the opsin (Nakanishi & Solomon, 1977).

The most characteristic bathorhodopsin lines in this region of the IR difference spectra are located at 1579 and 1536 cm^{-1} (Figures 2a+ and 3a+). The 1536-cm^{-1} bathorhodopsin line has been observed in resonance Raman spectra and has been assigned to an ethylenic mode of retinal (Oseroff & Callender, 1974; Sulkes et al., 1978). Evidence that the 1536-cm^{-1} B line in the IR spectra results from an ethylenic mode mixed with a 15-H in-plane bend is provided by its shift to 1529 cm^{-1} in the hydrated 15-^{2}H-labeled analogue pigment (Figures 2c+ and 3c+). This shift is in good agreement with resonance Raman studies [supplementary material from Eyring et al. (1982)] and IR spectra of protonated and deuterated butyl-

Table IV: Spectral Region between 1600 and 1500 cm^{-1}

		native[c]				15-^{13}C[d]				15-^{2}H[e]			
		B/I[f]		B/R		B/I		B/R		B/I		B/R	
species[a]	medium[b]	figure[g]	lines (cm^{-1})[h]	figure	lines (cm^{-1})	figure	lines (cm^{-1})	figure	lines (cm^{-1})	figure	lines (cm^{-1})	figure	lines (cm^{-1})
batho-rhodopsin (B)	H_2O	2a+	1579, 1536, <u>1518</u>	3a+	1579, 1536, <u>1520</u>	2b+	1578, 1534, <u>1520</u>	3b+	1578, 1534, <u>1515</u>	2c+	1577, 1529, (<u>1518</u>)	3c+	1575, 1529, (<u>1518</u>)
	$^{2}H_2O$	2d+	1582, 1538, (<u>1518</u>)	3d+	1584, 1536, <u>1518</u>	2e+	1580, 1534, <u>1519</u>	3e+	1581, 1534, <u>1518</u>	2f+	1582, 1529, (<u>1518</u>)	3f+	1583, 1581, 1531, (<u>1518</u>)
		native[c]				15-^{13}C[d]				15-^{2}H[e]			
		B/I[f]		I/R		B/I		I/R		B/I		I/R	
species[a]	medium[b]	figure[g]	lines (cm^{-1})[h]	figure	lines (cm^{-1})	figure	lines (cm^{-1})	figure	lines (cm^{-1})	figure	lines (cm^{-1})	figure	lines (cm^{-1})
iso-rhodopsin (I)	H_2O	2a−	1556, (1546)	4a+	1555, 1546	2b−	1555, 1547	4b+	1556, 1545	2c−	1558, 1540, (<u>1535</u>)	4c+	1555, (1540), <u>1535</u>
	$^{2}H_2O$	2d−	1556, (1546)	4d+	1556, (1546)	2e−	1558, (1546), 1511	4e+	1585, 1554, 1546	2f−	1556, 1545, (<u>1533</u>), 1511	4f+	1590, 1554, 1545, <u>1533</u>
		native[c]				15-^{13}C[d]				15-^{2}H[e]			
		B/R[f]		I/R		B/R		I/R		B/R		I/R	
species[a]	medium[b]	figure[g]	lines (cm^{-1})[h]	figure	lines (cm^{-1})	figure	lines (cm^{-1})	figure	lines (cm^{-1})	figure	lines (cm^{-1})	figure	lines (cm^{-1})
rhodopsin (R)	H_2O	3a−	1558, (1547), (1537), (1528)	4a−	(1558), (1547), 1537, 1528	3b−	1558, 1547, (1535), (1527), <u>1501</u>	4b−	1562, (1558), (1547), 1535, 1525	3c−	1560, 1542, (1535), (1527)	4c−	(1560), (1542). (1535), (1527)
	$^{2}H_2O$	3d−	1560, (1547), (1537), (1528), 1511	4d−	(1560), (1547), 1541, 1527	3e−	1558, (1547), (1538), (1526), 1511	4e−	(1558), (1547), 1538, 1526	3f−	1561, 1553, 1541, (1536), (1526), 1511	4f−	(1561), (1541), (1536), 1526

[a] The measured intermediate in the photosequence. [b] The media in which the ROS were suspended. The ROS suspended in H_2O yield hydrated films whereas the $^{2}H_2O$ media suspended ROS yield deuterated films. [c] Native ROS. [d] Pigments containing [15-^{13}C]retinal. [e] Pigments containing [15-^{2}H]retinal. [f] For example, B/I means the difference IR spectrum between B and I. [g] The (+) and (−) signs denote respectively the positive and negative sides of the difference spectra in the figures. [h] Lines that are weak and not discussed in the text are underlined; if the line is assigned in the text as belonging to a particular species but does not appear in both possible difference spectra, the line appears in parentheses for the figure in which it does not appear.

amine Schiff bases of *all-trans*-retinal (A. A. Croteau and K. Nakanishi, unpublished results). The 1579-cm^{-1} bathorhodopsin line has been detected in the resonance Raman studies of Narva & Callender (1980) and is fairly insenstive to deuteration and isotopic substitutions at C-15 (Figures 2b+, 3b+, 2c+, and 3c+). We propose that this 1579-cm^{-1} B line is a second, less intense, ethylenic mode of retinal.

For both isorhodopsin and rhodopsin more lines are seen in the IR in the region from 1600 to 1500 cm^{-1} than in the resonance Raman spectra. Inspection of isorhodopsin spectra (Figures 2a− and 4a+) indicates that isorhodopsin has lines in this region at 1556 (Figures 2a− and 4a+) and 1547 cm^{-1} (Figure 4a+, not seen in Figure 2a−; we argue that in this case the I 1547-cm^{-1} line is hidden under the more intense B 1536-cm^{-1} line). Rhodopsin has a line at 1558 cm^{-1} (Figure 3a−, but hidden under the I 1556-cm^{-1} line in Figure 4a−) and lines at 1537 and 1528 cm^{-1} (Figure 4a−, but hidden in Figure 2a− by the B 1536-cm^{-1} line). In addition, we propose that R, like I, has a line at 1547 cm^{-1} (although it does not appear in Figure 3a− or 4a−) on the basis of its similar behavior to the I 1547-cm^{-1} line upon isotopic substitution at C-15 (compare Figure 2b−, 2c− to Figure 3b−, 3c−).

These results, in which both R and I have lines at ca. 1556 and 1547 cm^{-1}, are consistent with the IR studies of unlabeled pigments by Siebert et al. (1983). However, resonance Raman studies detect a single line in this region for isorhodopsin at 1555 cm^{-1} and for rhodopsin at 1545 cm^{-1} (Callender et al., 1976; Mathies et al., 1977).

There are two plausible explanations for the existence of lines in this region of the IR spectrum, which are not present in the resonance Raman spectrum. The new IR lines could be amide or other protein (aspartate, glutamate, tyrosine) lines that appear due to small changes in the protein among isorhodopsin, rhodopsin, and bathorhodopsin. Alternately, these lines could be due to ethylenic modes of the retinal that are IR active but resonance Raman inactive. These two explanations can be distinguished. Isotopic substitutions within the chromophore are expected to affect only the vibrational modes of the chromophore whereas deuteration of the medium could in principle shift lines that arise from changes in either the chromophore or the protein.

The shift of the I and R 1547-cm^{-1} line to ca. 1540 cm^{-1} in the 15-^{2}H-labeled analogue pigment indicates that it is a chromophore line and thus a resonance Raman inactive ethylenic mode. Siebert et al. (1983) have speculated that this line in isorhodopsin might be due to a second ethylenic that is coupled to the C=N stretch, on the basis of the disappearance of this line in deuterated medium (compare Figure 4a+ and 4d+). However, one would expect a shift in this line in the 15-^{13}C-labeled pigments if the ethylenic and the C=N

stretching mode were coupled. Our IR data show no such shift of the 1547-cm^{-1} isorhodopsin and rhodopsin lines between native ROS and the 15-^{13}C-labeled pigment (Figures 2a−/2b−, 3a−/3b−, and 4a+/4b+). Furthermore, these R and I 1547-cm^{-1} lines do not shift between hydrated ROS and the deuterated 15-deuterated pigment analogues (compare Figures 2a−/2f−, 3a−/3f−, and 4a−/4f−), while they appear shifted to ca. 1540 cm^{-1} in the hydrated 15-deuterated pigments (compare Figures 2a−/2c−, 3a−/3c−, and 4a+/4c+). A similar shifting pattern is encountered in the FTIR of a methanolic solutions of simple retinal analogues (A. A. Croteau and K. Nakanishi, unpublished results), although it is at present not understood.

The line near 1556 cm^{-1} in both isorhodopsin and rhodopsin is fairly insensitive to deuteration of the medium and to isotopic substitution at C-15 (Figures 2−, 3−, and 4+). As mentioned above, this line has been previously observed (1555 cm^{-1}) in resonance Raman studies for isorhodopsin, but not rhodopsin, and assigned as an ethylenic mode in the isorhodopsin case.

A recent normal mode analysis of all-trans protonated Schiff bases of retinal identifies ethylenic modes at 1597, 1589, and 1563 cm^{-1} (Smith et al., 1985); ethylenic modes calculated at 1609 and 1568 cm^{-1} were not observed in these resonance Raman experiments. IR spectra yield lines at 1608 and 1557 cm^{-1} (A. A. Croteau and K. Nakanishi, unpublished results). The mode that has the largest resonance Raman intensity is located at 1563 cm^{-1} (Smith et al., 1985), whereas the largest IR intensity occurs at 1557 cm^{-1} (A. A. Croteau and K. Nakanishi, unpublished results). Our IR difference spectra indicate that ethylenic modes for rhodopsin may be located at 1558, 1547, 1537, and 1528 cm^{-1}, for bathorhodopsin at 1608, 1579, and 1536 cm^{-1}, and for isorhodopsin at 1556 and 1547 cm^{-1}.

Intensities of lines in resonance Raman spectra can be directly correlated with changes in equilibrium geometry upon electronic excitation (Callender & Honig, 1977; Warshel, 1977; Myers et al., 1982). Since upon absorption of light, rhodopsin (11-cis) is converted to bathorhodopsin (distorted all-trans), isorhodopsin (9-cis) to bathorhodopsin, and bathorhodopsin to both rhodopsin and isorhodopsin, the ground and excited states must involve appreciable changes in equilibrium geometry of the 11−12 bond in rhodopsin, the 9−10 bond in isorhodopsin, and both the 9−10 and 11−12 bonds in bathorhodopsin. This would imply that the 1545-cm^{-1} rhodopsin line contains appreciable C-11/C-12 character, the 1560-cm^{-1} isorhodopsin line appreciable C-9/C-10 character, and the 1536-cm^{-1} bathorhodopsin line appreciable contributions from C-9/C-10 and C-11/C-12.

Spectral Region between 1500 and 1400 cm^{-1}. In this region of the spectrum, lines are observed for rhodopsin and isorhodopsin at ca. 1453 cm^{-1} and for bathorhodopsin at 1435 cm^{-1} (Figures 2–4). These lines are observed both in H_2O and ^2H_2O and for all analogue pigments. In ^2H_2O, new lines appear for rhodopsin and isorhodopsin at ca. 1408 cm^{-1} and for bathorhodopsin at 1400 cm^{-1}. In resonance Raman (H_2O) experiments, rhodopsin is observed to have lines at ca. 1443 cm^{-1}, isorhodopsin at 1451 and 1420 cm^{-1}, and bathorhodopsin at 1437 cm^{-1} (Eyring et al., 1980; Narva & Callender, 1980). No assignment of these lines can be made at present.

Spectral Region between 1400 and 1100 cm^{-1} (Table V). The C–C stretches and C–C–H bends of the chromophore are expected to appear in the spectral region from 1400 to 1100 cm^{-1}. This region is commonly referred to as the fingerprint region of the retinal since the pattern of lines in this region has been found to be characteristic of the isomeric state (Callender et al., 1976; Mathies et al., 1977; Cookingham et al., 1978). Furthermore, the pattern of lines in this region remains relatively unperturbed when the isomers are incorporated into the protein environment of rhodopsin. For example, resonance Raman spectra of rhodopsin and isorhodopsin show patterns of lines that agree very favorably with the patterns of lines found in 11-*cis*-retinal and 9-*cis*-retinal, respectively. These similarities have provided further evidence that the chromophore in rhodopsin is the 11-cis isomer of retinal and in isorhodopsin is the 9-cis isomer (Callender et al., 1976; Mathies et al., 1977).

In the IR difference spectra a line is observed for bathorhodopsin at 1165 cm^{-1} (Figure 2a+ and 3a+) and for isorhodopsin at 1152 cm^{-1} (Figures 2a− and 4a+). The 1165-cm^{-1} bathorhodopsin line is of particular interest since it is characteristic of the all-trans isomer of retinal; an 1166-cm^{-1} line is observed in the resonance Raman and IR spectra of all-trans protonated Schiff bases (Braiman & Mathies, 1980; Mathies et al., 1977; A. A. Croteau and K. Nakanishi, unpublished results) and *all-trans*-retinals (Callender et al., 1976; Cookingham et al., 1978; Curry et al., 1982), and vibrational mode analysis has been used to assign it in *all-trans*-retinal to the C-10/C-11 stretch (Curry et al., 1982). Since the 1166-cm^{-1} line is characteristic of *all-trans*-retinal the existence of the 1166-cm^{-1} line in the IR resonance Raman spectra of bathorhodopsin provides further evidence that in bathorhodopsin the chromophore is an all-trans-like (transoid) isomer of retinal.

The 1166-cm^{-1} line in resonance Raman spectra of bathorhodopsin, however, has been a matter of some controversy. Eyring & Mathies (1979) detect a weak line for bathorhodopsin at 1166 cm^{-1}, while Aton et al. (1980) do not detect a line at this position. Lewis (1982) has criticized the ability to reliably detect such weak lines. However, since this line is of moderate intensity in the IR difference spectra, we believe the existence and position of this line are quite reliable. Furthermore, it does not shift appreciably upon isotopic substitution at C-15 (Figures 2b+, 2c+, 3b+, and 3c+) or deuteration of native or analogue ROS (Figures 2d+, 2e+, 2f+, 3d+, 3e+, and 3f+). In agreement with previous FTIR studies (Rothschild et al., 1983), we conclude that the behavior of the 1165-cm^{-1} bathorhodopsin line is consistent with its assignment to a C-10/C-11 stretch (Curry et al., 1982) and is furthermore indicative of the transoid nature of bathorhodopsin.

In isorhodopsin a line appears at ca. 1152 cm^{-1} in all the analogue spectra (Figures 2 and 4). This line compares well with a 1148-cm^{-1} line observed in the IR and resonance Raman spectra of 9-*cis*-retinals (Callender et al., 1976; Mathies et al., 1977; Cookingham et al., 1978). No line appears for rhodopsin in this region.

The pattern of B lines that appear between 1220 and 1190 cm^{-1} and their shifts upon isotopic substitution at C-15 are similar to line patterns observed in the resonance Raman and IR spectra of protonated and deuterated butylamine Schiff bases of *all-trans*-retinal (A. A. Croteau and K. Nakanishi, unpublished results; Smith et al., 1985). In this region of the spectrum, bathorhodopsin has lines at 1211 cm^{-1} (Figure 2a+, but hidden under the B 1207-cm^{-1} and R 1216-cm^{-1} lines in Figure 3a+) and 1207 cm^{-1} (Figure 3a+ but cancelled by the I 1207-cm^{-1} line in Figure 2a+), which upon ^{13}C substitution at C-15 behave in a manner analogous to lines in the resonance Raman spectra of protonated butylamine Schiff bases of *all-trans*-retinal at 1204 and 1191 cm^{-1}, respectively; the 1211-cm^{-1} B line does not shift upon isotopic substitution at C-15 (Figures 2+ and 3+) while the 1207-cm^{-1} line shifts to 1198 cm^{-1} upon ^{13}C substitution at C-15 (compare Figures 2a+ and 3a+ to Figures 2b+ and 3b+). This shift upon ^{13}C

Table V: Spectral Region between 1400 and 1100 cm^{-1}

		native[c]				15-^{13}C[d]				15-^{2}H[e]			
		B/I[f]		B/R		B/I		B/R		B/I		B/R	
species[a]	medium[b]	figure[g]	lines (cm^{-1})[h]	figure	lines (cm^{-1})	figure	lines (cm^{-1})	figure	lines (cm^{-1})	figure	lines (cm^{-1})	figure	lines (cm^{-1})
batho-rhodopsin (B)	H_2O	2a+	1352, 1332, 1322, 1307, 1286, 1277, 1246, 1240, 1223, 1211, (1207), 1165, 1110	3a+	1352, 1336, 1321, 1309, 1288, 1277, 1243, 1222, (1211), 1207, 1165, 1110	2b+	1352, 1336, 1322, 1306, 1286, 1278, 1246, 1222, 1211, 1198, 1167, 1110	3b+	1352, 1336, 1322, 1309, 1284, 1278, 1245, (1222), 1210, 1198, 1166	2c+	1352, 1325, 1307, 1286, 1274, 1244, 1220, 1211, 1204, 1169, 1112	3c+	1352, 1325, 1310, 1286, 1274, 1243, (1220), 1211, 1206, 1168
	$^{2}H_2O$	2d+	1350, 1336, 1322, 1307, 1285, 1277, 1242, 1222, 1212, (1207), 1166, 1112	3d+	1352, 1338, 1321, 1310, 1285, 1278, (1242), (1222), (1212), 1207, 1166, 1110	2e+	1360, 1337, 1322, 1308, 1286, 1278, 1245, 1222, 1212, 1198, 1167, 1111	3e+	1360, 1336, 1321, 1308, 1285, 1278, 1245, 1221, 1211, 1198, 1167, 1110	2f+	1352, 1327, 1308, 1290, 1272, 1247, 1238, 1222, 1212, 1203, 1170, 1110	3f+	1387, 1352, 1325, 1309, 1294, (1272), (1247), (1222), 1211, 1205, 1183, 1169, 1111

		native[c]				15-^{13}C[d]				15-^{2}H[e]			
		B/I[f]		I/R		B/I		I/R		B/I		I/R	
species[a]	medium[b]	figure[g]	lines (cm^{-1})[h]	figure	lines (cm^{-1})	figure	lines (cm^{-1})	figure	lines (cm^{-1})	figure	lines (cm^{-1})	figure	lines (cm^{-1})
iso-rhodopsin (I)	H_2O	2a-	1390, 1360, 1343, 1314, 1252, 1206, (1204), 1152	4a+	(1390), 1341, 1323, 1293, 1243, 1207, (1204), 1153	2b-	1390, 1360, 1343, 1314, 1265, 1254, 1204, 1191, 1153	4b+	(1390), 1370, 1342, 1317, 1256, 1240, 1204, 1192, 1153	2c-	1392, 1361, 1316, 1301, 1291, 1264, 1254, 1207, (1204), 1154	4c+	(1392), 1360, 1317, 1207, (1204), 1154
	$^{2}H_2O$	2d-	(1390), 1361, 1341, 1314, 1252, 1207, (1204), 1153	4d+	(1390), 1343, 1207, (1204), 1153	2e-	(1389), 1343, 1301, 1267, 1253, (1204), 1187, 1152	4e+	1389, 1341, 1317, 1295, 1254, 1245, 1204, 1192, 1155, 1142	2f-	1391, 1361, 1316, 1253, 1207, (1204), 1155	4f+	(1391), 1360, 1317, 1294, 1207, (1204), 1156

		native[c]				15-^{13}C[d]				15-^{2}H[e]			
		B/R[f]		I/R		B/R		I/R		B/R		I/R	
species[a]	medium[b]	figure[g]	lines (cm^{-1})[h]	figure	lines (cm^{-1})	figure	lines (cm^{-1})	figure	lines (cm^{-1})	figure	lines (cm^{-1})	figure	lines (cm^{-1})
rhodopsin (R)	H_2O	3a-	1390, 1360, 1345, 1328, 1316, 1251, 1238, 1216, 1191	4a-	1391, 1360, (1345), 1269, 1246, 1238, 1216, 1190	3b-	1390, 1363, 1343, 1315, 1300, 1294, 1264, 1253, 1231, 1215, 1188, 1185	4b-	1391, 1360, 1380, (1345), 1270, 1247, 1232, 1214, 1185	3c-	1393, 1367, 1316, 1301, 1265, 1249, 1227, 1216, 1157, 1151	4c-	1392, 1366, 1300, 1265, 1248, 1227, 1216

Table V (Continued)

		native[c]				15-^{13}C[d]				15-^{2}H[e]			
		B/R[f]		I/R		B/R		I/R		B/R		I/R	
species[a]	medium[b]	figure[g]	lines (cm^{-1})[h]	figure	lines (cm^{-1})	figure	lines (cm^{-1})	figure	lines (cm^{-1})	figure	lines (cm^{-1})	figure	lines (cm^{-1})
	$^{2}H_2O$	3d–	1365, 1345, 1302, 1270, 1252, 1238, 1232, 1218, 1195	4d–	1365 (1345), 1249, 1235, 1217, 1194	3e–	(1395), 1364, 1344, 1301, 1266, 1253, 1228, 1217, 1187, 1120	4e–	1395, 1365, (1345), 1326, 1272, 1265, 1235, 1229, 1216, 1187, 1176	3f–	1393, 1363, 1266, 1249, 1237, 1218	4f–	1393, 1367, 1301, 1266, 1249, 1237, 1220

[a] The measured intermediate in the photosequence. [b] The media in which the ROS were suspended. The ROS suspended in H_2O yield hydrated films whereas the $^{2}H_2O$ media suspended ROS yield deuterated films. [c] Native ROS. [d] Pigments containing [15-^{13}C]retinal. [e] Pigments containing [15-^{2}H]retinal. [f] For example, B/I means the difference IR spectrum between B and I. [g] The (+) and (–) signs denote respectively the positive and negative sides of the difference spectra in the figures. [h] Lines that are weak and not discussed in the text are underlined; if the line is assigned in the text as belonging to a particular species but does not appear in both possible difference spectra, the line appears in parentheses for the figure in which it does not appear.

substitution at C-15 is indicative that the 1207-cm^{-1} B line results from a normal mode, which contains a significant contribution from the C-14/C-15 stretch. However, this 1207-cm^{-1} bathorhodopsin line does not shift upward in the 15-deuterated pigment as would be expected on the basis of spectra of analogues of protonated retinal Schiff bases (A. A. Croteau and K. Nakanishi, unpublished results) or normal mode calculations (Smith et al., 1985).

Isorhodopsin has lines at 1207 (Figures 2a– and 4a+) and 1204 cm^{-1} (Figures 2b– and 4b+ but hidden under the 1207-cm^{-1} I line in Figure 2a– and 4a+), and rhodopsin has lines at 1191 and 1216 cm^{-1} (Figures 3a– and 4a–), which behave in a similar manner to B lines at 1207 and 1211 cm^{-1}, respectively. This analogy implies that the 1207-cm^{-1} I and 1191-cm^{-1} R lines also contain appreciable contributions from the C-14/C-15 stretch; however, the assignment of these lines awaits IR and resonance Raman studies of 11-cis and 9-cis model compounds.

The lines that have appreciable contributions from C-14/C-15 stretch, 1207 cm^{-1} in bathorhodopsin and isorhodopsin and 1191 cm^{-1} in rhodopsin, do not shift appreciably upon medium deuteration (compare Figure 3a+, 3d+ for bathorhodopsin, Figure 2a–, 2d– and Figure 4a+, 4d+ for isorhodopsin, and Figure 3a–, 3d– and Figure 4a–, 4d– for rhodopsin). These lines in 15-^{13}C-labeled pigments located at 1198 cm^{-1} in bathorhodopsin, 1191 cm^{-1} in isorhodopsin, and 1185 cm^{-1} in rhodopsin also do not shift appreciably upon medium deuteration (compare Figure 2b+, 2e+ for bathorhodopsin, Figure 2b–, 2e– and Figure 4b+, 4e+ for isorhodopsin, and Figure 4b–, 4e– for rhodopsin). Normal mode calculations have shown that for protonated Schiff bases having a C=N trans configuration the C-14/C-15 vibrational mode is expected to shift only a few wavenumbers upon medium deuteration, whereas for the C=N cis configuration this vibrational mode would shift to higher wavenumbers by about 60 cm^{-1} (Smith et al., 1984). The behavior of these lines suggest the trans or anti nature of the C=N bond in bathrhodopsin, rhodopsin, and isorhodopsin (Figure 5). The fact that the configuration of the C=N bond is unchanged in the primary photochemical event is consistent with what occurs in the bacteriorhodopsin system, in which both bacteriorhodopsin and its primary photoproduct K were found to have C=N trans configurations (Smith et al., 1984).

Siebert et al. (1983) have proposed that the rhodopsin line at 1238 cm^{-1} (Figures 3a– and 4a–) is due to the 15-H in-plane bend, on the basis of their observation that this line shifts to ca. 1250 cm^{-1} upon deuteration of the medium. As previously mentioned, small changes in temperature and/or humidity can cause base-line variation in this region of the spectrum, making identification of changes in amplitudes of lines in this area difficult. However, we did not observe a complete shift in this line upon deuteration of the medium, instead observing lines near 1251 and 1238 cm^{-1} in both hydrated (Figures 3a– and 4a–) and deuterated (Figures 3d– and 4d–) films albeit with some relative changes in intensity. In addition, we observe a strong 1248-cm^{-1} line in both hydrated and deuterated films for 15-deuterated pigments (Figures 3c–, 3f–, and 4c–, and 4f–) and a weak 1238-cm^{-1} line in the deuterated film of the 15-deuterated pigment (Figure 3f– and 4f–). These patterns are not consistent with the assignment of this line to the 15-H in-plane bend.

In bathorhodopsin a line at 1336 cm^{-1} (Figure 3a+, at 1332 cm^{-1} in Figure 2a+) disappears in 15-deuterated pigments (Figures 2c+, 2f+, and 3c+, 3f+) and a new line is observed at 995 cm^{-1} (Figures 2f+ and 3f+). In addition, upon 15-^{2}H substitution the intensity of the small 1352-cm^{-1} line (Figures 2a+ and 3a+ but not labeled) increases considerably (Figures 2c+, 2f+ and 3c+, 3f+). Similar shifts and intensity changes are observed for all-trans protonated butylamine Schiff bases (A. A. Croteau and K. Nakanishi, unpublished observations; Smith et al., 1985). Upon 15-^{2}H substitution, a line at 1343 cm^{-1} shifts to 988 cm^{-1} and a line at 1361 cm^{-1} increases in intensity.

We identify the 1336-cm^{-1} B line as the 15-H in-plane rock on the basis of its shift to 995 cm^{-1} for the 15-deuterated pigments. The 1361-cm^{-1} B line assignment is more problematic. Its gain in intensity in the 15-deuterated pigments suggests that it arises from a mode of the chromophore (possibly the 14-H in-plane rock), which is antisymmetrically coupled with the lower lying 15-H in-plane rock. However, one would expect that such a mode would also shift up in frequency when the coupling with the 15-H in-plane rock is removed by deuteration—a feature not observed for the 1361-cm^{-1} B line. Identification of the 1361-cm^{-1} B line therefore awaits the acquisition of a series of IR and resonance Raman spectra for analogues of all-trans protonated Schiff bases with various ^{2}H substitutions along the chain.

For both isorhodopsin and rhodopsin, lines are detected that behave in an analogous manner to the 1336- and 1361-cm^{-1} B lines. Lines at 1343 cm^{-1} for isorhodopsin and 1345 cm^{-1} for rhodopsin disappear and a new I line appears at 1000 cm^{-1} upon 15-^{2}H substitution (for I compare Figures 2a–/2c–,

2d−/2f−, 4a+/4c+, and 4d+/4f+ and note that the 1000-cm^{-1} I line is only clearly resolved in Figure 2c−, 2f−; for R compare Figure 3a−/3c− and 3d−/3f−) in a manner analogous to the 1336-cm^{-1} B line shift to 995 cm^{-1} upon 15-^2H substitution. Additionally, a new I line at 1361 cm^{-1} appears upon 15-^2H substitution (Figures 2c−, 2f− and 4c+, 4f+) while in rhodopsin a small line at ca. 1365 cm^{-1} increases considerably in intensity upon 15-^2H substitution (compare Figures 3a−/3c−, 3d−/3f−, 4a−/4c−, and 4d−/4f−). On the basis of the similar behavior upon 15-^2H substitution of the lines at 1343, 1345, and 1336 cm^{-1} in I, R, and B, respectively, we assign the 1343-cm^{-1} I and 1345-cm^{-1} R lines to their respective 15-H in-plane rocks.

Siebert et al. speculate that the 1391-cm^{-1} I and R lines in the B/I and B/R spectra, which are absent in ^2H_2O (compare Figures 2a− and 3a− to Figures 2d− and 3d−), are due to N–H in-plane bending modes (Siebert et al., 1983). The observation of a 1393-cm^{-1} rhodopsin line in the 15-deuterated B/R spectrum (Figure 3f−) shows that this assignment is not correct since upon deuteration the N–H bending mode should shift significantly. The bathorhodopsin lines at 1322, 1307, ca. 1286, 1277, ca. 1240–1246, 1222, and 1110 cm^{-1} are present in all the difference spectra (Figures 2+ and 3+), and hence, no assignments of these lines can be made on the basis of these studies.

Spectral Region between 1100 and 1000 cm^{-1}. The vibrational modes in the 1030–1000-cm^{-1} region have recently been assigned to the CH_3 in-plane rocking modes of retinal (Curry et al., 1982, 1985). [Data and analysis of various isomers of retinal have been published, whereas data and analysis have only been published for the all-trans form of retinal protonated Schiff bases (Smith et al., 1985).] For the all-trans, 9-cis, and 13-cis isomers a single strong line at 1008 cm^{-1} (1011 cm^{-1} for the 13-cis isomer) is observed. This line has been assigned to the symmetric coupled 9-CH_3, 13-CH_3 rock. This assignment implies that the two uncoupled CH_3 vibrations are nearly degenerate at ca. 1016 cm^{-1} and that they couple to form normal modes that are split apart by about 8 cm^{-1}, a strong line at 1008 cm^{-1} due to the symmetric combination and a line at 1024 cm^{-1} (of nearly zero intensity) for the antisymmetric combination. For the 11-cis isomer, lines at 1017 and 996 cm^{-1} are observed and have been assigned to the 9-CH_3 and 13-CH_3 rocks, respectively. The 9-CH_3 rock exhibits a normal isolated rock frequency, whereas the 13-CH_3 rock exhibits an anomalously low frequency. This result is in agreement with suggestions of Callender et al. (1976) that this low 13-CH_3 rock frequency is due to steric interactions between 13-CH_3 and 10-H in the 11-cis-12-trans chromophore.

Resonance Raman studies yield vibrational modes at 1006 cm^{-1} for bathorhodopsin, 1011 cm^{-1} for isorhodopsin, and 1018 and 997 cm^{-1} for rhodopsin. The 1018- and 997-cm^{-1} R lines have been assigned to the separate 9-CH_3 and 13-CH_3 rocks and the 1011-cm^{-1} I line to the symmetric coupled 9-CH_3 and 13-CH_3 rocks (Eyring et al., 1980).

The FTIR difference spectra show bathorhodopsin lines at 1021 and 1003 cm^{-1} (Figures 2a+ and 3a+), an isorhodopsin line at ca. 1013 cm^{-1} (Figures 2a− and 4a+), and a rhodopsin line at 997 cm^{-1} (labeled only in Figure 4c−). The positions of these lines are roughly independent of the isotopic substitution at C-15 and of deuteration of the medium. Our results for isorhodopsin and the lower frequency bathorhodopsin and rhodopsin lines are consistent with resonance Raman results. These IR and resonance Raman data, taken together, imply that in isorhodopsin and bathorhodopsin the two methyl rocks are degenerate in frequency, whereas in rhodopsin they are not. This is consistent with the additional interaction of the 13-CH_3 group in rhodopsin due to the 11-cis-12-s-trans conformation of the chromophore (Callender et al., 1976).

A rhodopsin line is detected at 1073 cm^{-1} (Figures 3a− and 4a−) whose position is independent of isotopic substitution at C-15 or deuteration of the medium. It is interesting to speculate on the origin of the 1073-cm^{-1} rhodopsin line. In 11-*cis*-retinal the 1084-cm^{-1} line has been assigned to the C-10/C-11 stretch. For the all-trans, 9-cis, 13-cis, and 9-cis,13-cis isomers the C-10/C-11 stretch is found at higher frequencies (1163, 1148, 1162, and 1144 cm^{-1}, respectively) (Curry et al., 1985). As pointed out by Curry (1984), this low frequency for the C-10/C-11 vibration in the 11-cis isomer is consistent with the observation of a 30–100-cm^{-1} decrease in the frequency of C–C stretches flanking the cis bonds of unsubstituted cis polyenes. Consistent with our assignment, resonance Raman experiments show a broad band at 1099 cm^{-1} for rhodopsin, whereas for isorhodopsin and bathorhodopsin no bands in the region 1100–1050cm^{-1} have been detected (Eyring et al., 1980).

Spectral Region between 1000 and 800 cm^{-1} (Table VI). It is in the 1000–800-cm^{-1} region of the spectrum that the hydrogen out of plane (HOOP) vibrations of retinal are found. The infrared spectra show lines unique to bathorhodopsin in the 800–1000-cm^{-1} region at 922, 908, 875, 853, 849, and 838 cm^{-1} (Figures 2a+ and 3a+). The 922- and 875-cm^{-1} bathorhodopsin lines do not shift appreciably upon deuteration of the ROS or isotopic substitution (^{13}C, ^2H) at C-15 of the retinal chromophore (compare Figures 2a+/2d+, 2a+/2d+/2c+, 3a+/3d+, and 3a+/3d+/3c+). This behavior is consistent with previous pigment analogue studies by resonance Raman spectroscopy from which the 922- and 875-cm^{-1} bathorhodopsin lines were assigned to the 11 and 10 hydrogen out of plane (HOOP) wagging modes, respectively (Eyring et al., 1982).

Eyring et al. (1982) have assigned the 853-cm^{-1} bathorhodopsin line to the 14 HOOP in part on the basis of their observation of a shift of this line to 859 cm^{-1} upon 15-deuteration. However, the IR B/I and B/R spectra show a new line at 859 cm^{-1} not only in the 15-deuterioretinal analogue spectra (compare Figures 2a+/2c+ and 3a+/3c+) but also for all the spectra of ROS analogues measured in ^2H_2O (Figures 2d+, 2e+, 2f+ and 3d+, 3e+, 3f+). In addition, the shoulder on the low-wavenumber side of this 859-cm^{-1} line seen in some of the spectra makes it difficult to say with certainty that the 853-cm^{-1} line disappears with the appearance of the 859-cm^{-1} line. This behavior makes assignment of the 853 line to the 14 HOOP wag questionable, since it is difficult to understand how this mode could be effected in the same manner by deuteration at either C-15 or the Schiff-base nitrogen.

The bathorhodopsin lines at 908, 849, and 838 cm^{-1} in the IR spectra have not been assigned. The 908-cm^{-1} B line disappears upon medium deuteration in both native and analogue ROS (compare Figures 2a+/2d+, 2b+/2e+, 2c+/2f+, 3a+/3d+, 3b+/3e+, and 3c+/3f+). We tentatively assign the 908-cm^{-1} B line to the N–H wag; however, it should be noted that this behavior would also be consistent with a vibrational mode of the protein involving an exchangeable proton. Eyring et al. (1982) have hypothesized the existence of an uncoupled 12 HOOP for bathorhodopsin around 830–860 cm^{-1}. Although current studies do not allow unequivocal assignment of this mode, peaks in the predicted positions at 838 and 849 cm^{-1} are indeed present in Figures 2+ and 3+. Consistent with assignment to the 12 HOOP, the 838-cm^{-1} line does not shift appreciably between native ROS and either [15-^{13}C]retinal, [15-^2H]retinal, or deuterated ROS analogues. The behavior of the 849-cm^{-1} line may be similar;

Table VI: Spectral Region between 1000 and 800 cm^{-1}

		native[c]				15-^{13}C[d]				15-^{2}H[e]			
		B/I[f]		B/R		B/I		B/R		B/I		B/R	
species[a]	medium[b]	figure[g]	lines (cm^{-1})[h]	figure	lines (cm^{-1})	figure	lines (cm^{-1})	figure	lines (cm^{-1})	figure	lines (cm^{-1})	figure	lines (cm^{-1})
batho-rhodop-sin (B)	H_2O	2a+	922, 907, 876, 851, 838	3a+	922, 908, 875, 853, 849, 840	2b+	921, 907, 875, 853, 848, 838	3b+	921, 909, 873, 851, 847, 840	2c+	922, 908, 874, 859, 851, 833, 791	3c+	922, 907, 874, 859, 848, 833, 791
	$^{2}H_2O$	2d+	921, 876, 858, 838	3d+	921, 872, 858	2e+	920, 874, 858, 841	3e+	920, 873, 857, 841	2f+	995, 921, 872, 859, 852, 840, 831	3f+	995, 920, 905, 872, 860, 847, 840, 830

		native[c]				15-^{13}C[d]				15-^{2}H[e]			
		B/I[f]		I/R		B/I		I/R		B/I		I/R	
species[a]	medium[b]	figure[g]	lines (cm^{-1})[h]	figure	lines (cm^{-1})	figure	lines (cm^{-1})	figure	lines (cm^{-1})	figure	lines (cm^{-1})	figure	lines (cm^{-1})
isorhodopsin (I)	H_2O	2a−	970, 958	4a+	(970), 959	2b−	967, 958	4b+	(967), 959	2c−	1000, 969, 959	4c+	(969), 959
	$^{2}H_2O$	2d−	970, 959	4d+	(970), 959	2e−	970, 958	4e+	(970), 959	2f−	1001, 967, 958	4f+	(967), 957

		native[c]				15-^{13}C[d]				15-^{2}H[e]			
		B/R[f]		I/R		B/R		I/R		B/R		I/R	
species[a]	medium[b]	figure[g]	lines (cm^{-1})[h]	figure	lines (cm^{-1})	figure	lines (cm^{-1})	figure	lines (cm^{-1})	figure	lines (cm^{-1})	figure	lines (cm^{-1})
rhodopsin (R)	H_2O	3a−	968	4a−	966	3b−	968	4b−	969	3c−	968	4c−	968
	$^{2}H_2O$	3d−	970	4d−	972	3e−	969	4e−	997, 975	3f−	972, 909	4f−	974

[a] The measured intermediate in the photosequence. [b] The media in which the ROS were suspended. The ROS suspended in H_2O yield hydrated films whereas the $^{2}H_2O$ media suspended ROS yield deuterated films. [c] Native ROS. [d] Pigments containing [15-^{13}C]retinal. [e] Pigments containing [15-^{2}H]retinal. [f] For example, B/I means the difference IR spectrum between B and I. [g] The (+) and (−) signs denote respectively the positive and negative sides of the difference spectra in the figures. [h] Lines that are weak and not discussed in the text are underlined; if the line is assigned in the text as belonging to a particular species but does not appear in both possible difference spectra, the line appears in parentheses for the figure in which it does not appear.

unfortunately, its behavior is obscured by the appearance of the 859-cm^{-1} line in the cases of deuterated ROS and [15-^{2}H]retinal analogues (Figures 2c+, 3c+, 2d+, and 3d+). The 859-cm^{-1} line in these cases seems to have a shoulder that could be due to either the 853- or the 849-cm^{-1} line. If the shoulder is due to the 849-cm^{-1} line, the 849-cm^{-1} line could be assigned as the 12 HOOP mode. The line that is not assigned to the 12 HOOP could also be due to a HOOP mode of the chromophore not observed in resonance Raman experiments. It is intriguing to speculate that the additional line is the antisymmetric combination of the 7–8 coupled HOOP.

The existence of an uncoupled 12-H HOOP for bathorhodopsin has been attributed to a specific protein–substrate interaction (Eyring et al., 1982), a suggestion in agreement with the double point-charge model (Honig et al., 1979). Recently, it has been suggested that the uncoupled 12-H HOOP may be due to steric interaction of the 12-H with the 9-CH_3 hydrogens due to a proposed 10-s-cis conformation for bathorhodopsin (Liu & Asato, 1985). We believe this interpretation to be unlikely since the C-10/C-11 stretch would be considerably lower in the 10-s-cis conformation than the 10-s-trans conformation. The C-10/C-11 stretch occurs at 1165 cm^{-1} in bathorhodopsin and at 1170 cm^{-1} in protonated Schiff bases of *all-trans*-retinal (Smith et al., 1985).

An additional feature of the IR spectra of bathorhodopsin remains unexplained. In the 15-^{2}H-labeled pigment in both hydrated and deuterated media, a new B line appears at 833 cm^{-1} (Figures 2c+, 2f+ and 3c+, and 3f+). It seems unlikely that this line could be the 15-^{2}H out of plane wag since it is expected at lower frequencies (ca. 790 cm^{-1}), and although the signal to noise in the 700-cm^{-1} region of these IR spectra is poor, we detect what appears to be a new 796-cm^{-1} B line in the 15-^{2}H-labeled pigment (see Figures 2c+ and 3c+). The assignment of the new 833-cm^{-1} B line in the 15-^{2}H-labeled pigments therefore remains unanswered. We tentatively assign the new 796-cm^{-1} B line to the 15-^{2}H out of plane wag.

The B/R and I/R difference spectra show a rhodopsin line at ca. 970 cm^{-1} (Figures 3a− and 4a−). This line does not shift appreciably in deuterated ROS (Figures 3d− and 4d−) or upon isotopic substitution at C-15 (Figures 3b−, 3c− and 4b−, 4c−), in good agreement with the Eyring et al. (1982) assignment of the 970-cm^{-1} rhodopsin line to the 11-H/12-H HOOP mode.

The I/R spectra show a line for isorhodopsin at 959 cm^{-1} (Figure 4+), while the B/I spectra show two lines for isorhodopsin at ca. 959 and 970 cm^{-1} (Figure 2−). These patterns are the same in all the analogues. A rationalization for this pattern is that isorhodopsin has bands at both 959 and 970 cm^{-1} while rhodopsin also has an absorption at 970 cm^{-1} that is more intense. This 959-cm^{-1} isorhodopsin line has been observed in resonance Raman and assigned to the coupled 7-H/8-H HOOP (Eyring et al., 1982). Resonance Raman studies do not clearly show the presence of a 970-cm^{-1} isorhodopsin line; however, in the resonance Raman studies of Marcus & Lewis (1979), the broad 960-cm^{-1} I line has a pronounced shoulder at 970 cm^{-1}. It is likely that the 970-cm^{-1} IR line in isorhodopsin is due to the 11-H/12-H HOOP mode; however, this assignment places the HOOP's for hydrogens

both trans (in isorhodopsin) and cis (in rhodopsin) to the 11–12 double bond at the same frequency, which is somewhat puzzling.

Discussion

The results of this study have corroborated many of the conclusions reached through resonance Raman studies. Our IR spectra show the existence of an 1165-cm^{-1} bathorhodopsin line, thus providing further evidence that the retinal of bathorhodopsin is transoid. In the 1660-cm^{-1} Schiff-base region, comparisons of line positions in hydrated and deuterated media of native ROS and its 15-^{13}C and 15-^{2}H analogues (Table III) clearly show that the Schiff-base linkage is protonated in rhodopsin, bathorhodopsin, and isorhodopsin. Furthermore, the observation that no line in the Schiff-base region disappears upon deuteration of the medium indicates that the protonated C=N stretching frequency is the same in all three species, also in agreement with previous resonance Raman results. The lack of appreciable shifts in the C-14/C-15 vibrational modes (at ca. 1200 cm^{-1}) upon medium deuteration is interpreted in terms of the protonated Schiff base having a C=N trans conformation in all three species. Furthermore, the position of the C-10/C-11 stretch in bathorhodopsin (1165 cm^{-1}) is indicative of a 10-s-trans conformation. These results indicate that the primary effect of light on rhodopsin is an 11-cis/11-trans isomerization.

While most of the lines in the IR spectra that are due to retinal modes agree favorably in both position and behavior upon isotopic substitution with lines in the resonance Raman spectra, there are several notable exceptions. First, resonance Raman results show a single ethylenic for isorhodopsin at 1555 cm^{-1} and for rhodopsin at 1545 cm^{-1}, but the IR spectra show two lines at 1560 and 1547 cm^{-1} in both isorhodopsin and rhodopsin. Second, in the HOOP region of the resonance Raman spectra a single line is observed for isorhodopsin at 959 and at 969 cm^{-1} for rhodopsin, whereas in the IR spectra two lines are observed at 959 and 969 cm^{-1} for isorhodopsin.

Although the above differences and similarities are intriguing, the major strength of IR spectroscopy is its ability to detect changes in the protein and lipid during these early stages of the photosequence. The IR spectra presented show many lines that are not observed in resonance Raman spectra. While some of these lines may be retinal modes that are resonance Raman inactive, we believe that many of these new lines are indeed due to changes in the protein and/or lipid. It seems clear from this early work that significant changes in both the protein conformation and environment of specific amino acid residues (aspartic and glutamic acids) occur in even the first steps of the rhodopsin photosequence. For example, as shown schematically in Figure 5, it is reasonable to suspect that isomerization of the 11–12 double bond in the conversion of rhodopsin to bathorhodopsin would cause changes in the environment of the amide bonds (1700–1500-cm^{-1} region) to which lysine-296 is linked. Similarly, the conversion should lead to changes in the COO^{-}/COOH groups in the vicinity of the protonated Schiff-base linkage. The exact nature of these changes has yet to be elucidated.

Acknowledgments

We thank R. Callender, B. Honig, R. Masel, R. Mathies, and L. Stryer for helpful discussions, L. Zimanyi for his contribution to the early phases of these experiments, and B. Nelson for ROS preparations and high-performance liquid chromatography determinations.

Registry No. PSB, 32798-55-3; 11-*cis*-[15-^{13}C]retinal, 97905-67-4; 11-*cis*-[15-^{2}H]retinal, 97905-68-5; [1-^{13}C]acetic acid, 1563-79-7; isobutylene, 115-11-7; [1-^{13}C]acetic acid *tert*-butyl ester, 93834-82-3; trans–cis C-18 ketone, 25529-03-7; 11-*cis*,13-*cis*-*tert*-butyl[15-^{13}C]retinoate, 97827-64-0; 11-*cis*-*tert*-butyl[15-^{13}C]retinoate, 97905-69-6; 11-*cis*-[15-^{13}C]retinol, 97827-65-1; 11-*cis*,13-*cis*-[15-^{13}C]retinol, 97905-70-9; 11-*cis*,13-*cis*-[15-^{13}C]retinal, 97905-71-0; *trans*-[15-^{2}H]retinal, 75238-14-1.

References

Akita, H., Tanis, S. P., Adams, M., Balogh-Nair, V., & Nakanishi, K. (1980) *J. Am. Chem. Soc. 102*, 6370–6372.

Alben, J. O., & Fiamingo, F. (1985) in *Physical Techniques in Biological Research* (Rousseau, D. L., Ed.) Academic Press, New York.

Applebury, M. L., Peters, K. S., & Rentzepis, P. M. (1978) *Biophys. J. 23*, 375–382.

Aton, B., Doukas, A. G., Narva, D., Callender, R. H., Dinur, U., & Honig, B. (1980) *Biophys. J. 29*, 79–94.

Bagley, K., Dollinger, G., Eisenstein, L., Singh, A. K., & Zimanyi, L. (1982) *Proc. Natl. Acad. Sci. U.S.A. 79*, 4972–4976.

Bagley, K., Dollinger, G., Eisenstein, L., Vittitow, J., Zimanyi, L., Ebrey, T. G., & Nelson, B. (1983) *Biophys. J. 41*, 337a.

Bagley, K., Dollinger, G., Eisenstein, L., Hong, M., Vittitow, J., & Zimanyi, L. (1984) in *Information and Energy Transduction in Biological Membranes* (Bolis, C. L., Helmreich, E. J. M., & Passow, H., Eds.) pp 27–37, Liss, New York.

Balogh-Nair, V., & Nakanishi, K. (1982) in *New Comprehensive Biochemistry* (Tamm, Ch., Ed.) Vol. 3, pp 283–334, Elsevier Biomedical Press, Amsterdam.

Birge, R. R. (1981) *Annu. Rev. Biophys. Bioeng. 10*, 315–354.

Braiman, M., & Mathies, R. (1980) *Biochemistry 19*, 5421–5428.

Callender, R., & Honig, B. (1977) *Annu. Rev. Bioeng. 6*, 33–55.

Callender, R. H., Doukas, A., Crouch, R., & Nakanishi, K. (1976) *Biochemistry 15*, 1621–1629.

Cookingham, R. E., Lewis, A., & Lemley, A. T. (1978) *Biochemistry 17*, 4699–4711.

Crouch, R., Purvin, V., Nakanishi, K., & Ebrey, T. G. (1975) *Proc. Natl. Acad. Sci. U.S.A. 72*, 1538–1542.

Curry, B. (1984) Ph.D. Thesis, University of California, Berkeley, CA.

Curry, B., Broek, A., Lugtenburg, J., & Mathies, R. (1982) *J. Am. Chem. Soc. 104*, 5274–5286.

Curry, B., Palings, I., Broek, A. D., Pardoen, J. A., Lugtenburg, J., & Mathies, R. (1985) *Adv. Infrared Raman Spectrosc.* (in press).

Ebrey, T. G. (1982) *Methods Enzymol. 88*, 516–521.

Eyring, G., & Mathies, R. (1979) *Proc. Natl. Acad. Sci. U.S.A. 76*, 33–37.

Eyring, G., Curry, B., Mathies, R., Fransen, R., Palings, I., & Lugtenburg, J. (1980) *Biochemistry 19*, 2410–2418.

Eyring, G., Curry, B., Broek, A., Lugtenburg, J., & Mathies, R. (1982) *Biochemistry 21*, 384–393.

Hargrave, P. A., McDowell, J. H., Curtis, D. R., Wang, J. K., Juszczak, E., Fong, S.-L., Rao, J. K. M., & Argos, P. (1983) *Biophys. Struct. Mech. 9*, 235–244.

Hartzell, S. L., Sullivan, D. E., & Rathke, M. (1974) *Tetrahedron Lett.*, 1403–1406.

Honig, B., Dinur, U., Nakanishi, K., Balogh-Nair, V., Gawinowicz, M. A., Arnabaldi, M., & Motto, M. G. (1979) *J. Am. Chem. Soc. 101*, 7084–7086.

Hubbard, R., & Kropf, A. (1958) *Proc. Natl. Acad. Sci. U.S.A. 44*, 130–139.

Kakitani, H., Kakitani, T., Rodman, H., Honig, B., & Callender, R. (1983) *J. Phys. Chem. 87*, 3620–3628.

Kates, M., & Kushawa, S. C. (1978) in *Energetics and Structure of Halophilic Microorganisms* (Caplan, S. R., & Ginzbourg, M., Eds.) pp 461–478, Elsevier/North-Holland, Amsterdam.

Langworthy, T. A., Tornabene, T. G., & Holzer, G. (1982) *Zentralbl. Bakteriol., Mikrobiol. Hyg., Abt. 1, Orig. C: 3*, 228–244.

Lewis, A. (1978) *Proc. Natl. Acad. Sci. U.S.A. 75*, 549–553.

Lewis, A. (1982) *Methods Enzymol. 88*, 561–617.

Lewis, A., Fager, R. S., & Abrahamson, E. W. (1973) *J. Raman Spectrosc. 1*, 465–470.

Liu, R. S. H., & Asato, A. E. (1985) *Proc. Natl. Acad. Sci. U.S.A. 82*, 259–263.

Marcus, M. A., & Lewis, A. (1979) *Photochem. Photobiol. 29*, 699–702.

Mathies, R., Oseroff, A. R., & Stryer, L. (1976) *Proc. Natl. Acad. Sci. U.S.A. 73*, 1–5.

Mathies, R., Freedman, T. B., & Stryer, L. (1977) *J. Mol. Biol. 109*, 367–372.

Myers, A. B., Mathies, R. A., Tannor, D., & Heller, E. J. (1982) *J. Chem. Phys. 77*, 3857–3866.

Nakanishi, K., & Solomon, P. M. (1977) *Infrared Absorption Spectroscopy*, Holden-Day, San Francisco.

Narva, D., & Callender, R. H. (1980) *Photochem. Photobiol. 32*, 273–276.

Ono, N., Yamada, T., Saito, T., Tanaka, K., & Kaji, A. (1978) *Bull. Chem. Soc. Jpn. 51*, 2401–2404.

Oseroff, A. R., & Callender, R. H. (1974) *Biochemistry 13*, 4243–4248.

Ottolenghi, M. (1980) *Adv. Photochem. 12*, 97–200.

Ovchinnikov, Y. A., Abdulaev, N. G., Fegina, M. Y., Artamontov, I. D., Zolotarev, A. S., Kostina, M. B., Bogachuk, A. J., Moroshnikov, A. I., Martinov, V. I., & Kudelin, A. B. (1982) *Bioorg. Khim. 8*, 1011–1014.

Papermaster, D. S., & Dreyer, W. J. (1974) *Biochemistry 13*, 2438–2444.

Peters, K., Applebury, M. L., & Rentzepis, P. M. (1977) *Proc. Natl. Acad. Sci. U.S.A. 74*, 3119–3123.

Rosenfeld, T., Honig, B., Ottolenghi, M., Hurley, J., & Ebrey, T. (1977) *Pure Appl. Chem. 49*, 341–351.

Rothschild, K. J., & Marrero, H. (1982) *Proc. Natl. Acad. Sci. U.S.A. 79*, 4045–4049.

Rothschild, K. J., Zageski, M., & Cantore, W. A. (1981) *Biochem. Biophys. Res. Commun. 103*, 483–489.

Rothschild, K. J., Sanches, R., & Clark, N. A. (1982) *Methods Enzymol. 88*, 696–714.

Rothschild, K. J., Cantore, W. A., & Marrero, H. (1983) *Science (Washington, D.C.) 219*, 1333–1335.

Shichi, H. (1983) *Biochemistry of Vision*, Academic Press, New York.

Siebert, F., & Mäntele, W. (1980) *Biophys. Struct. Mech. 6*, 147–164.

Siebert, F., & Mäntele, W. (1983) *Eur. J. Biochem. 130*, 565–573.

Siebert, F., Mäntele, W., & Gerwert, K. (1983) *Eur. J. Biochem. 136*, 119–127.

Smith, S. O., Myers, A. B., Pardoen, J. A., Winkel, C., Mulder, P. P. J., Lugtenburg, J., & Mathies, R. (1984) *Proc. Natl. Acad. Sci. U.S.A. 81*, 2055–2059.

Smith, S. O., Myers, A. B., Mathies, R. A., Pardoen, J. A., Winkel, C., von der Berg, E. M. M., & Lugtenburg, J. (1985) *Biophys. J.* (in press).

Sulkes, M., Lewis, A., & Marcus, M. A. (1978) *Biochemistry 17*, 4712–4722.

Suzuki, T., & Callender, R. H. (1981) *Biophys. J. 34*, 261–265.

Van der Meer, K., Mulder, J. J. C., & Lugtenburg, J. (1976) *Photochem. Photobiol. 24*, 363–367.

Wald, G., & Brown, P. K. (1950) *Proc. Natl. Acad. Sci. U.S.A. 36*, 84–92.

Warshel, A. (1977) *Annu. Rev. Biophys. Bioeng. 6*, 273–300.

Yoshizawa, T., & Wald G., (1965) *Nature (London) 197*, 1279–1286.

Zawadski, M. E., & Ellis, A. B. (1983) *J. Org. Chem. 48*, 3156–3161.